
Grokking Group Multiplication with Cosets

Dashiell Stander¹ Qinan Yu^{1,2} Honglu Fan^{1,3} Stella Biderman¹

Abstract

We use the group Fourier transform over the symmetric group S_n to reverse engineer a 1-layer feed-forward network that has "grokked" the multiplication of S_5 and S_6 . Each model discovers the true subgroup structure of the full group and converges on circuits that decompose the group multiplication into the multiplication of the group's conjugate subgroups. We demonstrate the value of using the symmetries of the data and models to *understand* their mechanisms and hold up the "coset circuit" that the model uses as a fascinating example of the way neural networks implement computations. We also draw attention to current challenges in conducting mechanistic interpretability research by comparing our work to Chughtai et al. [6] which alleges to find a different algorithm for this same problem.

1. Introduction

The program of modern mechanistic interpretability was first clearly articulated in [44]: deep neural networks use directions in neuron activation space as features and perform tasks by combining those features in neural "circuits." The features that neural networks learn and the circuits that they form do not have to be opaque. With care and effort researchers can peer into the black box of deep models and understand *how* they accomplish the tasks that they are trained to accomplish.

We follow prior work in circuit-level mechanistic interpretability and study a model and a task that we can understand completely [6, 23, 40, 41]. In so doing we hope to build an understanding of the types of features that neural networks form and the precise mechanisms with which neural networks combine and transform those features. We hope that by reverse-engineering the function of each neuron in a model that performs a simple task we will contribute to a foundation of understanding from which to study the mechanisms of massive models.

¹EleutherAI ²Brown University ³University of Geneva. Correspondence to: Dashiell Stander <dash.stander@gmail.com>.

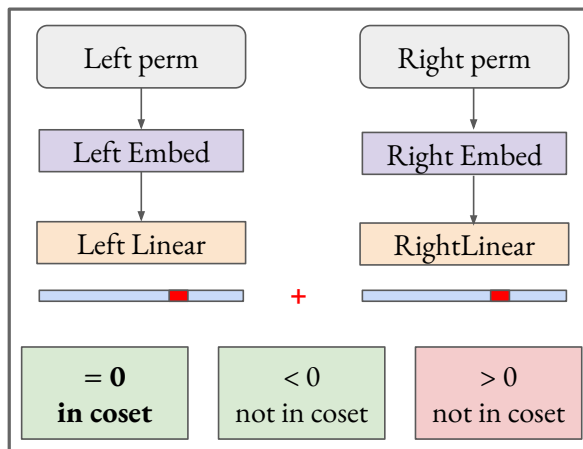


Figure 1. The coset circuit that the model uses to perfectly generalize the group multiplication. The circuit stores information about coset membership for the left and right permutations in the embeddings. The linear layer queries the embeddings and combines the information to determine whether or not the product is in a specific coset. Coset membership is encoded in the sign of the activations.

In this paper we return to the subject of Chughtai et al. [6] and analyze one hidden layer fully connected networks of varying widths that have perfectly learned the task of group multiplication. We found their analysis incomplete, however, and build on it by using the full Group Fourier transform to **completely** reverse-engineer the most common mechanism converged networks use to implement group multiplication. Though there are in fact many different neural circuits that the networks form, we can describe the vast majority using the cosets of S_n that we refer to as the *coset circuit*. Cosets are subsets of a group that have specific properties in relation to each other that the model can use to perfectly generalize in the task of group multiplication (see Section 3.1 for concrete examples of cosets for permutation groups or Appendix D for a formal definition).

The high level steps of the coset circuit, given two permutations σ_l, σ_r , are:

1. In the left and right embedding layers, the model stores information about membership in dozens of left and right cosets.

2. In the linear layer, the embeddings are queried to get the coset membership for σ_l and σ_r . The linear layer combines this information to get the probable coset membership of their product $\sigma_l\sigma_r$.
3. In the unembedding layer, the identity of $\sigma_l\sigma_r$ is determined as the only permutation in S_n that satisfies all of the different coset memberships computed by the linear layer in step 2.

1.1. Our Contributions

Our main contributions are as follows:

1. We completely reverse engineer a 1-hidden layer fully-connected network trained on the permutation groups S_5 and S_6 .
2. We present a novel application of the Group Fourier Transform to circuit-level mechanistic interpretability.
3. We apply a methodology inspired by Geiger et al. [21] to use causal interventions thoroughly test all of the properties of our proposed circuit.
4. We survey current research in mechanistic interpretability and draw connections between the difficulty of our work and broader challenges in the field.

2. Related Work

Mechanistic Interpretability We analyze the mechanisms of neural networks at the *circuit level* of individual and small groups of neurons, drawing directly on the work of [40, 41, 45, 59]. Our work builds directly on “A Toy Model of Universality” by Chughtai et al. [6]. We recreated precisely their experimental setup for the groups S_5 and S_6 , but found their analysis incomplete and could not find a mechanism implementing their proposed “Group Composition via Representations” algorithm. For a thorough comparison of our work and [6], see Appendix F.

Grokking Our choice of studying models trained on small permutation groups was made in no small part because of the appearance of “grokking,” wherein the model first memorizes a training set and then much later generalizes to the held out data perfectly. Grokking was first identified by Power et al. [47] and has been well studied for its counter-intuitive training dynamics [31, 38, 52, 49, 57, 56]. We conducted all the analysis on fully grokked models with perfect test accuracy.

Group Theory Our analysis owes much to the seminal monograph “Group Representations in Probability and Statistics” [12] and the varied literature building on it [8, 30, 29, 26, 28]. We implement in Pytorch the Fast Fourier transform algorithm over the symmetric group S_n

developed by Clausen & Baum [7]. Our implementation is heavily inspired by the example in Julia of Plumb et al. [46].

3. Background

3.1. Permutations and the Symmetric Group

In this section we will give a concrete exposition of some concepts of group theory as they are concretely realized in the permutation groups that we study. For a more formal introduction to group theory, please refer to Appendix D.

A permutation of n elements is a map σ that sends one ordering of the n elements to a different ordering, for example the order-reversing permutation on four elements would be:

$$(1\ 2\ 3\ 4) \xrightarrow{\sigma} (4\ 3\ 2\ 1)$$

and the identity permutation, denoted e , changes nothing:

$$(1\ 2\ 3\ 4) \xrightarrow{e} (1\ 2\ 3\ 4)$$

We write specific permutations by identifying them with the image of their action on the elements $\{1, 2, \dots, n\}$ in their standard order. For the above example, we would simply denote the order reversing permutation on four elements as $(4\ 3\ 2\ 1)$.

We multiply two permutations on n elements σ, τ by composition, read from right to left. If $\sigma = (4\ 3\ 2\ 1)$ and $\tau = (3\ 2\ 1\ 4)$, then $\sigma\tau$ is the permutation we obtain by first applying τ and then applying σ :

$$(1\ 2\ 3\ 4) \xrightarrow{\tau} (3\ 2\ 1\ 4) \xrightarrow{\sigma} (4\ 1\ 2\ 3)$$

What we see is that first applying τ and then σ has the same effect as just applying the permutation $(4\ 1\ 2\ 3)$. Additionally every permutation σ has an inverse σ^{-1} such that $\sigma\sigma^{-1} = e$. These properties makes all of the permutations on n elements a *group* called the symmetric group, which we write S_n .

There are six permutations in S_4 that “fix” 4:

$$\begin{matrix} (1\ 2\ 3\ 4) & (2\ 1\ 3\ 4) & (3\ 2\ 1\ 4) \\ (1\ 3\ 2\ 4) & (3\ 1\ 2\ 4) & (2\ 3\ 1\ 4) \end{matrix}$$

These six permutations form a *subgroup* of S_4 because multiplying any two permutations that fix four results in another permutation that fixes four. You can see that these six permutations are homomorphic to S_3 by simply “forgetting” about the 4 that is fixed in the fourth position.

If we take a subgroup such as the copy of $S_3 < S_4$ that fixes four and multiply every element of that subgroup on

the left by some element $\sigma \in S_4$ then we get a *left coset* of S_3 denoted σS_3 . The transposition $\tau = (4\ 2\ 3\ 1)$ switches the elements in the first and fourth positions. The elements of τS_3 are:

$$\begin{pmatrix} 4 & 2 & 3 & 1 \\ 4 & 3 & 2 & 1 \end{pmatrix} \quad \begin{pmatrix} 4 & 1 & 3 & 2 \\ 4 & 1 & 2 & 3 \end{pmatrix} \quad \begin{pmatrix} 4 & 2 & 1 & 3 \\ 4 & 3 & 1 & 2 \end{pmatrix}$$

This coset is characterized by every element having 4 in the first position, because τ switches positions the first and fourth positions and S_3 always has 4 in the fourth position. We would get a coset with all of the elements of S_4 with 4 in the third position if we multiplied S_3 the left by the transposition that switches three and four.

There are also *right cosets* where every element in a subgroup is multiplied from the right. The elements of $S_3\tau$ are:

$$\begin{pmatrix} 4 & 2 & 3 & 1 \\ 4 & 3 & 2 & 1 \end{pmatrix} \quad \begin{pmatrix} 1 & 4 & 3 & 1 \\ 3 & 4 & 2 & 1 \end{pmatrix} \quad \begin{pmatrix} 3 & 2 & 4 & 1 \\ 2 & 3 & 4 & 1 \end{pmatrix}$$

This right coset is characterized by every element having 1 in the fourth position, because S_3 fixes the element in the fourth position and τ has 1 in the fourth position.

There are in fact four subgroups of S_4 that are isomorphic to S_3 : one where each element $\{1, \dots, 4\}$ is fixed. In general there are n subgroups of S_n that are isomorphic to S_{n-1} . These different ‘‘copies’’ of $S_3 < S_4$ are all *conjugate* to each other. Conjugation by an element σ maps $x \mapsto \sigma x \sigma^{-1}$. So if we have the S_3 that we have been working with that fixes 4 and conjugate by $\sigma = (1\ 4\ 3\ 2)$, then $\sigma S_3 \sigma^{-1}$ is the copy of S_3 that fixes 2:

$$\begin{pmatrix} 1 & 2 & 3 & 4 \\ 1 & 2 & 4 & 3 \end{pmatrix} \quad \begin{pmatrix} 3 & 2 & 1 & 4 \\ 4 & 2 & 1 & 3 \end{pmatrix} \quad \begin{pmatrix} 4 & 2 & 3 & 1 \\ 3 & 2 & 4 & 1 \end{pmatrix}$$

If a subgroup is invariant to conjugation then it is a *normal* subgroup. The only normal subgroup of S_n for $n > 4$ is the *alternating group* A_n of even permutations.

A transposition is a permutation $\tau \in S_n$ that switches (‘‘transposes’’) two elements $i, j \in [n]$ and leaves the remaining elements fixed. Every element of S_n can be decomposed into a product of transpositions. For a given permutation this decomposition is not unique, but the number of transpositions in the decomposition is constant. The permutations that have an even number of transpositions are referred to as ‘‘even’’ permutations and those with an odd number are ‘‘odd.’’ A_n is made up of the permutations that have an even number of transpositions. For normal subgroups the left and right subgroups are equal, so $\sigma A_n = A_n \sigma$.

We will mostly refer to groups by name, but we will denote a general group as capital G and a general subgroup as

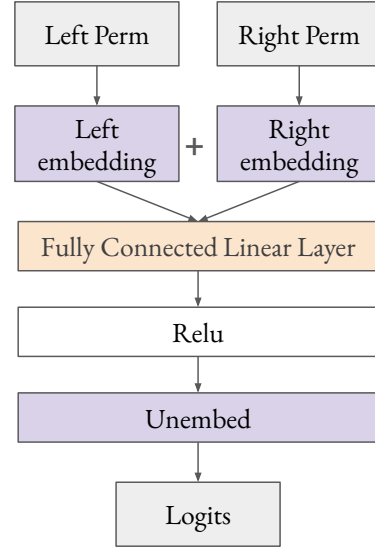


Figure 2. Model Architecture: we follow the model architecture used by [6]. The one-hot vectors of left and right permutations pass through separate embeddings. We concatenate the embeddings and pass them through a single fully-connected hidden layer with ReLU activations. An unembedding matrix transforms the activations into logits.

$H \leq G$. For a proper subgroup ($H \neq G$), we will write $H < G$. For a normal subgroup, we will use $N \trianglelefteq G$.

3.2. Fourier Transform over Groups

The Discrete Fourier Transform (DFT) converts a function f defined on $\{0, 1, \dots, n-1\}$ to a complex-valued function via the formula:

$$\hat{f}(k) = \sum_{t=0}^{n-1} f(t) e^{-2i\pi kt/n}, \quad k \in \{0, \dots, n-1\}$$

The DFT is commonly interpreted as a conversion from the *time* domain to the *frequency* domain because the $e^{-2i\pi kt/n}$ terms define a complex sinusoid with frequency $2\pi kt/n$. The frequency domain in this case means that these frequencies provide an alternative orthonormal basis from which we can work with functions. A function on $\{0, 1, \dots, n-1\}$ can be represented as a vector $f = (x_0 \ x_1 \ \dots \ x_{n-1})^\top$ and its basis is given by the identity matrix I_n . The DFT defines a basis transformation, much like any other. The Fourier basis is given n vectors. The first basis vector, corresponding to $k = 0$, is all ones. The $k = 1$ basis vector is $(1 \ e^{-2i\pi/n} \ \dots \ e^{-2i\pi(n-1)/n})$, and all of the rest for up to $n-1$ are given by $(1 \ e^{-2i\pi k/n} \ \dots \ e^{-2i\pi(n-1)k/n})$.

This basis has a number of useful properties, that stem from how well-fit it is to the structure of the domain. There are

many functions that appear complicated in the time domain that are relatively simple or sparse in the frequency domain.

The DFT has a particularly nice interpretation as a function on the cyclic group C_n , which is isomorphic to addition modulo n . Please refer to Appendix D or to references such as [12, 19, 30] for a more detailed discussion.

The interpretation of the DFT as being over the cyclic groups can be generalized to non-commutative groups. We go over the construction in Appendix D.6 and E. The high level interpretation, however, is the same. For functions from $S_n \rightarrow \mathbb{C}$ there is an orthonormal basis that is equivariant to translations and convolutions. The frequencies for the Fourier transform over S_n are given by the partitions of n . The “highest” frequencies can be interpreted as representing functions that are constant on permutations that all agree on a small number of elements of $[n]$ [16].

4. Model Architecture

We study a fully connected feed-forward network that is trained to learn the multiplication of finite permutation groups. As shown in Figure 2, the model contains separate left and right embeddings, followed by a fully connected linear layer with ReLU activations, and an unembedding layer.

- One hot vectors \mathbf{x}_g with length $|G|$.
- Two embedding matrices, \mathbf{E}_l , \mathbf{E}_r with dimensions $(d, |G|)$, where d is embedding dimension.
- A linear layer \mathbf{W} with dimension $(w, 2d)$, w denoting the width of the linear layer. After the linear layer we apply the ReLU pointwise nonlinearity.
- An unembedding layer \mathbf{U} with dimension $(|G|, w)$, which transforms the outputs of the ReLU and linear layer to into logit space for the group.

We also note that the first d columns of the linear layer will only act on the left embeddings and the second d columns will only act on the right embeddings, so we can analyze \mathbf{W} as the concatenation of two (w, d) matrices: $\mathbf{W} = [\mathbf{L} \ \mathbf{R}]$.

$$\mathbf{W} \begin{bmatrix} \mathbf{E}_l \mathbf{x}_g \\ \mathbf{E}_r \mathbf{x}_h \end{bmatrix} = \mathbf{L} \mathbf{E}_l \mathbf{x}_g + \mathbf{R} \mathbf{E}_r \mathbf{x}_h$$

5. Coset Circuits

In this section we will describe the precise mechanism of the *coset circuits* that the models use to implement multiplication in S_5 and S_6 .

First in Section 5.1 we will describe how in the linear layer the simplest circuit, the “Sign Circuit,” implements the multiplication of the two cosets of the alternating group A_n .

In Section 5.2 we will describe how the linear layer uses coset information with *conjugate* subgroups such as $S_4 < S_5$.

And in Section C.3 we discuss the distribution of different circuits and subgroups that the model converges on over many different runs.

5.1. Sign Circuit

The even permutations form a subgroup called the alternating group A_n . A_n has two cosets: the group itself A_n and all of the odd permutations τA_n . The sign map sgn is given by:

$$\text{sgn}(\sigma) = \begin{cases} 1 & \sigma \in A_n \\ -1 & \sigma \in \tau A_n \end{cases}$$

The sign map respects multiplication in S_n . For any $\sigma, \rho \in S_n$, the sign of their product is the product of their signs: $\text{sgn}(\sigma\rho) = \text{sgn}(\sigma) \text{sgn}(\rho)$.

There are three steps to each neuron’s mechanism. In what follows, x is the magnitude of the pre-activation, σ refers to a permutation, and the subscripts l, r, t on σ either refer to the left input permutation, the right input permutation, or the target permutation $\sigma_t = \sigma_l \sigma_r$, respectively.

1. The neuron weights corresponding to the left and right permutations “read off” the pre-activations from the embeddings. The pre-activations for the left and right take on one of two values: $x \text{sgn}(\sigma)$ or $-x \text{sgn}(\sigma)$.
2. The left and right pre-activations are added together through linear layer, so that the full pre-activations now take on one of three values: $-2x, 0$, or $2x$.
3. The ReLU activation function cuts off the pre-activations if they are $-2x$ and otherwise passes them along unchanged to the unembedding layer.

Let us take as a concrete example the neuron shown in Fig. 3, where the left pre-activations $L(\sigma) = -\text{sgn}(\sigma)x$ and the right pre-activations $R(\sigma) = \text{sgn}(\sigma)x$. The full action of the neuron is given by $\max(0, L(\sigma_l) + R(\sigma_r))$ and there are three cases:

1. $\text{sgn}(\sigma_l) = \text{sgn}(\sigma_r) \Rightarrow \text{sgn}(\sigma_l \sigma_r) = 1$. In this case $L(\sigma_l)$ and $R(\sigma_r)$ destructively interfere, cancelling out to 0. Both the pre-activation and activation are 0.
2. $\text{sgn}(\sigma_l) = -1, \text{sgn}(\sigma_r) = 1 \Rightarrow \text{sgn}(\sigma_l \sigma_r) = -1$. In this case $L(\sigma_l)$ and $R(\sigma_r)$ reinforce each other and sum to a positive value. Since $2x > 0$, the activation value is $2x$.

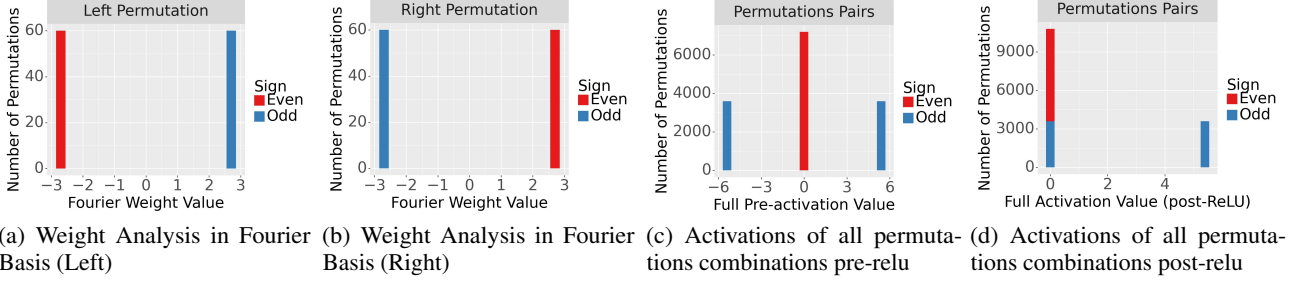


Figure 3. Four subfigures in two subgroups

- 3. $\text{sgn}(\sigma_l) = 1, \text{sgn}(\sigma_r) = -1 \Rightarrow \text{sgn}(\sigma_l\sigma_r) = -1$. Like in (2) the product $\sigma_l\sigma_r$ is an odd permutation and $L(\sigma_l)$ and $R(\sigma_r)$ constructively interfere, though this time $L(\sigma_l) + R(\sigma_r) = -2x < 0$. Thus ReLU clips the pre-activation and sends it to 0, so despite the information that $\sigma_l\sigma_r$ is even is present in the pre-activations, the activation that gets passed to the unembedding layer is identical to an even permutation as in (1).

5.2. Conjugate Subgroup Circuit

All four ways to multiply two cosets of A_n are well-defined. For each of the four options (even-even, odd-even, etc...) we know which coset of A_n the product will be in, but no other subgroup of S_n has this property. What they have are other conjugate subgroups. The model learns to identify those subgroups using the fact that the coset multiplication is well-defined for specific pairs of conjugate subgroups. In table 1 we provide the coset multiplication table for two subgroups of S_5 that we will refer to as H_1 and H_5 . Both are isomorphic to S_4 , H_1 fixes 1 and H_5 fixes 5. They are related by conjugation. The transposition $\tau_{(15)}$ sends one subgroup to the other: $\tau_{(15)}H_1\tau_{(15)} = H_5$ and $\tau_{(15)}H_5\tau_{(15)} = H_1$.

Far from being fully defined for every combination, every right coset of H_5 has precisely one paired left coset of H_1 that produces the coset $H_1\tau_{(15)}$. $H_1\tau_{(15)}$ has 24 elements, but the because of the double coset structure of

Despite this being more complicated for us to reason about than the A_5 case, the neural network treats these cases the same. There are pairs of subgroups that have a predictable multiplication, for a specific neuron the model learns features so that the pre-activations of the predictable products precisely cancel out to zero, and when that neuron fires the models knows that the product is *not* in the coset that neuron is specialized to predict.

5.3. Decoding Permutations with Coset Membership

The unembedding layer receives as input a vector of activations from that encode the coset membership of of the product $\sigma_l\sigma_r$. Each element of this vector can best be thought

	H_1	$\tau_{(12)}H_1$	$\tau_{(13)}H_1$	$\tau_{(14)}H_1$	$\tau_{(15)}H_1$
H_5					$\tau_{(15)}H_1$
$H_5\tau_{(15)}$	$\tau_{(15)}H_1$				
$H_5\tau_{(25)}$		$\tau_{(15)}H_1$			
$H_5\tau_{(35)}$			$\tau_{(15)}H_1$		
$H_5\tau_{(45)}$				$\tau_{(15)}H_1$	

Table 1. Coset multiplication table for H_1, H_5 where $H_i := \{\sigma \in S_5 \mid \sigma(i) = i\}$. The coset $\tau_{(15)}H_1$ corresponds to all of the permutations in S_5 with 1 in the fifth position. If the space is left blank, then multiplication of those two cosets creates every element of S_5 *not* in $\tau_{(15)}H_1$.

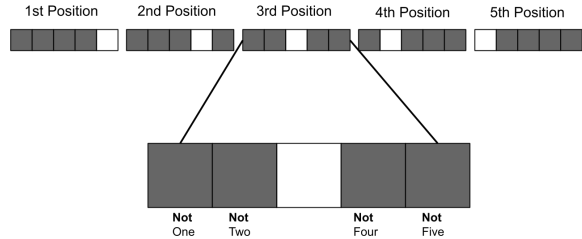


Figure 4. An example of an $S_4 < S_5$ coset circuit bit pattern for the permutation (5 4 3 2 1). The value of each position of the permutation is encoded in five coset circuits, twenty-five in total. Highlighted is the code for the third position. The value is 3 because three is the only circuit for that position that did *not* fire. Each individual circuit for a position-value pair (i.e. a single square in the diagram) will consist of as few as one or as many as fifteen neurons dedicated. The median number of neurons involved in a single coset circuit depends on the subgroup, but is around four.

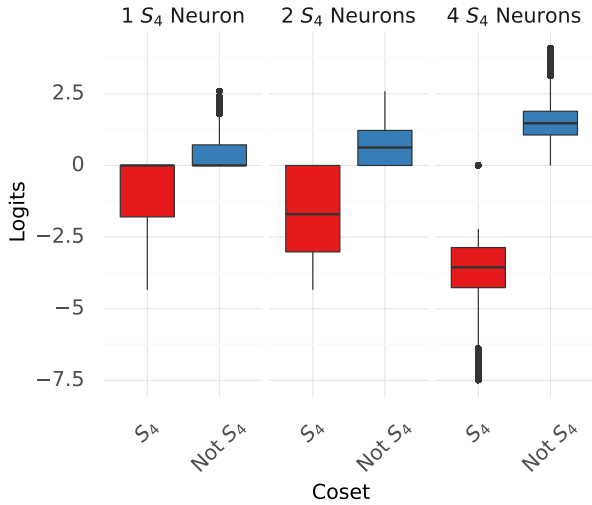


Figure 5. The effect of combining coset circuits. These show the contributions of one, two, and all four S_4 coset circuits to the logits of each permutation when the target permutation is *not* in S_4 (when the target is in S_4 then none of these neurons fire and their contributions to the logits is identically zero).

of as an on/off switch keyed to a specific coset. If the activation is positive then the product $\sigma_l \sigma_r$ is certainly not in that coset, but if it is zero it is only *probably* in the coset. Putting aside this ambiguity for a moment, we can see that with enough of these circuits the model can uniquely encode every permutation $\sigma \in S_n$ and perfectly solve the group multiplication.

Take as an example the five subgroups $H_i < S_5$ that fix the element i and are isomorphic to S_4 . For any pair (H_i, H_j) , including when $i = j$, there is a double coset consisting of all permutations that have i in the j^{th} position. As shown in Figure 4, we can associate five circuits to each position of the product permutation $\sigma_l \sigma_r$. The zoomed in portion of Figure 4 shows the five circuits that correspond to the 3rd position. Each circuit encodes the information “is the value in the 3rd position i ?” If the circuit fires then the answer to that question is “no,” but there will always be one circuit of the five that does not fire. Encoded in this way, the membership in all 25 circuits *uniquely identifies* every permutation in S_5 . In general, because the cosets of a subgroup partition the entire group, if there are k conjugate subgroups of $H \leq G$, then the k^2 shared cosets will uniquely identify each element of G .

The actual single-neuron coset circuits are not perfect on/off switches. Because of the ReLU half of the time the neuron does not fire (refer to Figure 3(d) and notice the large amount of even permutations with 0 activation). The model compensates for this by having multiple neurons dedicated to a single coset. Figure 5 shows how the unembedding

layer aggregates four distinct (H_1, H_1) circuits. For each of the neurons the effects on the final logits is simple: the product $\sigma_l \sigma_r$ is not in H_1 , so the the unembedding uses the signal from these neurons to decrease the logits of all of the permutations in H_1 and increase the logits of all of the permutations that are in H_1 . For a single neuron, however, there is non-trivial overlap between H_1 and not- H_1 at 0. The mistakes of each individual neuron cancel out when they are all added together, a single neuron may fail to activate for a permutation, but it is very unlikely that all four (H_1, H_1) neurons will fail to fire for that neuron. As we see in Figure 5, with all four neurons there is minimal overlap in the logits.

6. The Process of Reverse Engineering

In this section, we recite the process of reverse engineering the coset circuit. First, we observe the activations and build up a theory for their mechanism. Second, we confirm the sufficiency and necessity of the circuits we have identified via ablations. Finally, we rigorously validate our hypothesis by testing the properties of the circuit through causal interchange interventions.

6.1. Identifying Coset Circuits

To do mechanistic interpretability you must spend some time staring at the weights. The group Fourier transform did, however, give us a place to start looking. Individual neurons would concentrate entirely on irreducible representations of S_n , the “frequencies” of the group Fourier transform. It was as if the activations of each neuron were a pure sine wave, as in [40]. Harmonic analysis over S_n is subtler than in the classical case, however, and this was not enough for us to propose a concrete mechanism. After extensive manual effort and many dead-ends, we realized that a single neuron had its activations concentrated on the cosets of F_{20} , the Frobenius group of order 20 [14]. All of the activations for permutations in the same coset had the same value, with very little variance. This was so strange and unexpected that it warranted further investigation, which ultimately led us to discover the coset circuit.

For a function $f : G \rightarrow \mathbb{R}$, let $C_H(f)$ denote the the degree to which f concentrates on the cosets $H \leq G$ where:

$$C_H(f) := \frac{\sum_{gH} \text{Var}[f|_{gH}]}{\text{Var}[f]}$$

Explicitly $C_H(f)$ calculates the degree to which restricting to the cosets of H reduces the variance of f , $C_H(f) < 1$ implies that f can meaningfully be understood better by looking at the values that it takes on cosets. Since S_5 only has 156 subgroups¹, it is tractable to do an exhaustive search

¹Verified with Sage [50] and GAP [20].

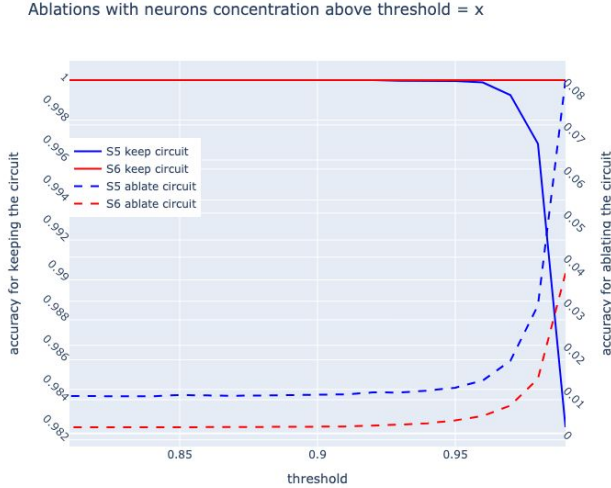


Figure 6. Ablation: Two cases of ablation. The full lines indicate ablating the double coset circuits in S_5 and S_6 , the dashed lines indicate ablating the other neurons that don’t form the double coset circuits.

and calculate

$$\operatorname{argmin}_{H \in \text{Sub}(G)} C_H(f)$$

the subgroup that minimizes the variance of f for every neuron in the model.

6.2. Ablations

To validate that the coset circuit is not only sufficient but also necessary to implement multiplication in S_n , we conduct ablations to observe the change in accuracy at inference time in two different ways: when the identified circuit is ablated and when the rest of the network is ablated.

If the identified circuit is necessary to solve the task, then we expect to see a drop in the accuracy when the identified circuit is removed from the network. If it is additionally the primary circuit used by the model, we expect the accuracy to remain high when we ablate the rest of the neurons and only keep the ones that form the coset circuits.

In figure 6, we observe a similar trend in both cases of ablations in both S_5 and S_6 . We selected neurons that concentrate on one irrep above the threshold of x percent. When we only keep the neurons that have a concentration higher than 90%, the accuracy remains perfect in S_6 over 24 runs with various model sizes. The accuracy is near perfect (0.982) in S_5 over 107 runs. However, when we ablate these neurons, the accuracy drop to only 0.04 in S_6 and 0.08 in S_5 . This aligns with our initial hypothesis suggesting that the coset circuits are necessary and sufficient.

We also observe that the performance of S_5 (blue line) has a

higher variance than S_6 (red line) We hypothesize that this is due to the smaller model sizes used in S_5 .

6.3. Causal Interventions

To rigorously test the properties of the coset circuit, we carefully designed *causal interchange interventions* [21] targeting the properties of different components in the circuits. We need to confirm that our model of the circuit serves as a faithful causal abstraction for the behavior of the actual neural circuit. We aggregated runs over 128 S_5 models of different and recorded their average loss and accuracy. Initially, over the initial models without intervention, we have accuracy extremely close to 1.

Embedding Exchange The left and right embeddings encode different information—membership in right and left cosets, respectively—and cannot be interchanged. To test this we intervene to switch the left and right embeddings. After the intervention, we observed a significant drop in accuracy to 0 and a rise in loss. This aligns with our expectation that the membership is an important property that can’t be switched.

Switch Permutation Sign The pre-activations are symmetric about the origin and the sign of the pre-activations does not matter, only whether or not the pre-activations is equal to zero. The *relative* sign of the left and right pre-activations should matter a lot. To test this, we have three tests: changing the sign of just the left embeddings, just the right embeddings, and both embeddings. In the case where we change both the sign and with commutative property, we can still expect the left and right activation to cancel out. Therefore, we should see a near-perfect accuracy and near-0 loss. The result is as expected. When we change the sign of only the left or right embedding, such cancellation law doesn’t hold anymore. Therefore, we observe a 0 accuracy in both cases.

Absolute Value Non-linearity The circuit can create a perfect 0-1 coset membership switch with multiple neurons on constructive interference, but every single neuron is noisy and fundamentally limited by the ReLU non-linearity. To test this, we replace the ReLU activation function with the absolute value function $x \mapsto |x|$. We observe perfect accuracy and an even lower loss that a half of the original loss.

ReLU Clip If the pre-activations are greater than zero and aren’t filtered by the ReLU, then the magnitude of the activations does not matter, there is no particular information in or distinction between a small or large pre-activation value. To test this, we patch the activations of neurons only when they are greater than some small constant and replace

Intervention	Mean Accuracy	Mean Loss
Base Model	0.9999	1.97e-6
Embedding Swap	0.01	4.76
Switch Left and Right Sign	1	1.97e-6
Switch Left Permutation Sign	0	22.39
Switch Right Permutation Sign	0	22.36
Perturb $\mathcal{N}(0, 0.1)$	0.9999	2.96e-6
Perturb $\mathcal{N}(0, 1)$	0.978	0.0017
Absolute Value Non-Linearity	1	3.69e-13
Perturb $\mathcal{N}(1, 1)$	0.88	0.029
Perturb $\mathcal{N}(-1, 1)$	0.98	0.0021

Table 2. Causal interventions aggregated over 128 runs on S_5 with different sizes

them with a normally distributed value centered around the mean activation of that neuron.

Distribution Change It is essential to the functioning of each neuron that a large proportion of the pre-activations are close to zero. To test this we compare how adding noise from a $\mathcal{N}(-1, 1)$ and $\mathcal{N}(1, 1)$ affect the performance of the model. We can see that changing the distribution of the activation in Perturb $\mathcal{N}(-1, 1)$ changes the performance less significantly than $\mathcal{N}(1, 1)$. This indicates that the coset requires 0 as a threshold value to decide the membership.

The results of these interventions can be viewed in Table 2

7. Discussion

7.1. Communication and Replication in Mechanistic Interpretability

The project of mechanistic interpretability strives to understand and explain inner workings of a machine learned model. As the large models that are popular today are immensely complicated and difficult to deconstruct, a substantial amount of mechanistic interpretability research is dedicated to either small models or work that allows insights gleaned from small models to be extended to larger models.

Unfortunately, our analysis reveals that even allegedly simple cases can be very challenging to get right. By revising the problem considered by Chughtai et al. [6] and finding drastically different mechanisms after extensive and earnest effort, our work reveals how challenging it can be to get the full picture correct. We refer the reader to Appendix F for a full side-by-side comparison of our work with Chughtai et al. [6].

Based on our analysis of twelve mechanistic interpretability papers [6, 9, 11, 22, 24, 25, 37, 40, 41, 55, 58, 59] we have identified five core steps in mechanistic interpretability work:

1. Pick a reference data set or distribution that is correlated to the task.
2. Identify a subset of nodes in the model’s computation graph that acts as a neural circuit such that the activations of the circuit are causally connected to the reference distribution.
3. Establish that this circuit accounts for some substantial portion of the performance on the task.
4. Come up with a model of the circuit that faithfully abstracts the its functionality.
5. Causally test that the behavior of your model is faithful across data distributions.

Many new techniques for accomplishing step 2 such as activation and path patching [22, 53, 55] have been developed, though in our case we relied on the spectral properties of permutation groups to tell us where to stark looking. As [55] discuss, step 3 can also be difficult in larger models.

Steps 4 and 5 are a difficult, manual, and largely ad-hoc process. Once we have pinpointed the subset of neurons that is doing something important we still need to interpret what it is doing: what information those neurons are encoding, the precise mechanism with which those neurons act and are acted upon by the rest of the network, etc...

We believe that the root issue with [6] is that they could not find a precise mechanism for matrix-matrix multiplications in a 1-layer network. They got to step 4 and came up with a compelling theory that fit the evidence and tied in nicely with prior work such as [3, 40]. Without a concrete and detailed theory for how the model implements their proposed algorithm their ability to move on to step 5 and confirm that the network behaves as they predict is limited. Our work and that of [6] together are a case study in why performing detailed and circuit-specific tests is necessary. The spectral evidence in the weights and logs that both of

our teams found did not uniquely determine a single circuit, but was consistent with both the GCR algorithm and the coset circuit. **It was only after performing the causal interchange interventions detailed in Section 6.3 that we were confident that we understood what the model was doing.**

We believe that one of the most promising paths forward for making step 5 as easy and rigorous as possible is extending the work of Geiger et al. [21]. There is a long history of interpretability techniques giving inconsistent and misleading evidence [1, 4, 13, 27], and recent results show that the most modern techniques can be vulnerable to similar issues [5, 18, 25, 34, 37]. There are ways to mitigate those weaknesses and in our review of the literature we were encouraged to see that most projects people went to great lengths to causally test specific features of the circuits that they propose under a variety of data distributions. Until we have developed better tools to make performing these tests easier, however, their application will remain ad hoc.

There is another subtler issue caused by the difficulty of communicating the precise mechanisms of neural circuits once they have been identified. Lieberum et al. [32] talk about the dilemma they faced when describing the circuits they found with pseudocode: they could remain faithful to the matrix algebra the circuit uses or provide an understandable, high-level explanation, but struggled to do both. In our work we have opted to keep our explanations as concrete and close to the actual neurons as possible, but doing so in a way that people will actually understand has been difficult. Effective communication of every minor detail and tweak to our architecture, such as concatenating the embeddings of the left and right permutations, is crucial for our audience to properly understand the circuit we are trying to explain. We need to develop better and more specific jargon, a grammar for communicating the circuits we find in a way that other researchers can understand. We know that the researchers who are doing the research can be fooled by explanations, but the situation for people reading and reviewing interpretability research is even worse. Our experience doing this project and writing this paper has led us to believe that developing a concise language for communicating our theories and the circuits we find is essential for facilitating progress in interpretability.

Finally, even simple examples can give rise to immense complexity. In Zhang et al. [58] the authors show that which algorithm a network learns can be sensitive to details of the experimental set-up such as the learning rate and initialization. While we were able to exactly replicate the results of Chughtai et al. [6] due to precise reporting, the release of their code, and personal communication, it is unfortunately common for machine learning researchers to not fully report their experimental set-up or release all of their evaluation ar-

tifacts. In such settings, it may be impossible to distinguish between different results due to genuinely different model behaviors versus ones due to erroneous analysis.

7.2. Spectral Information and Grokking

There is now a growing body of work making links between models in highly constrained domains that exhibit perfect generalization and the domain-appropriate Fourier transform. Nanda et al. [40] find that models trained on modular addition encode the dual representation of the cyclic group C_p directly and Barak et al. [3] hypothesize that the model is using the spectral gap calculated via the Fourier transform on the Boolean cube inherent to the noisy sparse parities problem. We now find that a 1-hidden-layer network uses Fourier-sparse functions to solve multiplication on permutation groups. There are known results from complexity and computational learning theory that functions with low-degree Fourier concentration are, in a precise sense, “learnable” [42]. Though this still does not provide direct evidence of a link, we find it intriguing and an exciting direction for future research.

7.3. Duality and Interpretable Bases

Though the precise connections between the learning dynamics, the spectral characteristics of the weights, and the generalization properties of the model remain opaque, it is absolutely the case that this project would have been much more difficult (and perhaps impossible) without an interpretable basis from which to view the weights and activations.

The Fast Fourier Transform (FFT) [10] is widely regarded as one of the most important algorithms of all time. The generalizations of harmonic analysis to more complex geometries has also been integral to physics in the last century [2]. It is not surprising that similar algorithms would prove invaluable in machine learning and mechanistic interpretability.

There is also a rich representation theory of semigroups and monoids [51] and existing work describing FFTs for inverse semigroups [35, 36]. It appears promising that the surprising results of Liu et al. [33] might become concretely interpretable via the representation theory of the monoids that they study.

8. Conclusion

In this paper we performed an a circuit level analysis to discover the concrete mechanism a one layer fully connected network uses to solve group multiplication in S_5 and S_6 . We showed that the model decomposes S_5 and S_6 into its cosets and uses that structural information to perfectly implement the task. We related how we found the circuit using the Group Fourier Transform and our methodology for con-

firming that our model of the circuit was faithful to its true behavior. Finally, we surveyed some modern research in mechanistic interpretability, their methodologies and the types of evidence they use to confirm their work. The causal interchange analysis that was crucial for us to confirm our hypotheses is difficult to perform and, to our knowledge, has not been applied to a real-world problem. This is an important obstacle for future research to overcome.

Acknowledgements

We would like to thank Coreweave for donating the computing resources that we used to run all of our experiments and to Bilal Chughtai for helpful discussions we had throughout the project. We would also like to thank Nora Belrose, Aidan Ewart, Hailey Schoelkopf, and Cédric Simal for their helpful feedback on an earlier draft of this paper.

References

- [1] Adebayo, J., Gilmer, J., Muelly, M., Goodfellow, I., Hardt, M., and Kim, B. Sanity checks for saliency maps, 2020.
- [2] Atiyah, M. F. Duality in mathematics and physics, 2007. URL https://fme.upc.edu/ca/arxius/butlleti-digital/riemann/071218_conferencia_atiyah-d_article.pdf.
- [3] Barak, B., Edelman, B. L., Goel, S., Kakade, S., Malach, E., and Zhang, C. Hidden Progress in Deep Learning: SGD Learns Parities Near the Computational Limit, January 2023. URL <http://arxiv.org/abs/2207.08799>. arXiv:2207.08799 [cs, math, stat].
- [4] Bolukbasi, T., Pearce, A., Yuan, A., Coenen, A., Reif, E., Viégas, F., and Wattenberg, M. An interpretability illusion for bert, 2021.
- [5] Casper, S., Li, Y., Li, J., Bu, T., Zhang, K., Hariharan, K., and Hadfield-Menell, D. Red teaming deep neural networks with feature synthesis tools, 2023.
- [6] Chughtai, B., Chan, L., and Nanda, N. A Toy Model of Universality: Reverse Engineering How Networks Learn Group Operations. Technical Report arXiv:2302.03025, arXiv, May 2023. URL <http://arxiv.org/abs/2302.03025>. arXiv:2302.03025 [cs, math] type: article.
- [7] Clausen, M. and Baum, U. Fast Fourier Transforms for Symmetric Groups: Theory and Implementation. *Mathematics of Computation*, 61(204): 833–847, 1993. ISSN 0025-5718. doi: 10.2307/2153256. URL <https://www.jstor.org/stable/2153256>. Publisher: American Mathematical Society.
- [8] Cohen, T. and Welling, M. Group Equivariant Convolutional Networks. In *Proceedings of The 33rd International Conference on Machine Learning*, pp. 2990–2999. PMLR, June 2016. URL <https://proceedings.mlr.press/v48/cohenc16.html>. ISSN: 1938-7228.
- [9] Conmy, A., Mavor-Parker, A. N., Lynch, A., Heimersheim, S., and Garriga-Alonso, A. Towards Automated Circuit Discovery for Mechanistic Interpretability, October 2023. URL <http://arxiv.org/abs/2304.14997>. arXiv:2304.14997 [cs].
- [10] Cooley, J. W. and Tukey, J. W. An algorithm for the machine calculation of complex fourier series. *Mathematics of computation*, 19(90):297–301, 1965.
- [11] Davies, X., Nadeau, M., Prakash, N., Shaham, T. R., and Bau, D. Discovering variable binding circuitry with desiderata, 2023.
- [12] Diaconis, P. *Group Representations in Probability and Statistics*, volume 11 of *Institute of Mathematical Statistics Lecture Notes*. Institute of Mathematical Statistics, Hayward, CA, 1988. ISBN 0-940600-14-5.
- [13] Doshi-Velez, F. and Kim, B. Towards a rigorous science of interpretable machine learning, 2017.
- [14] Dummit, D. S. and Foote, R. M. *Abstract Algebra*. Wiley, 3rd edition, July 2003. ISBN 978-0-471-43334-7.
- [15] Elias M. Stein, R. S. *Fourier analysis: an introduction*. Princeton lectures in analysis 1. Princeton University Press, 2003. ISBN 069111384X,9780691113845.
- [16] Ellis, D., Friedgut, E., and Pilpel, H. Intersecting Families of Permutations, July 2017. URL <http://arxiv.org/abs/1011.3342>. arXiv:1011.3342 [math].
- [17] Erdos, P. On an elementary proof of some asymptotic formulas in the theory of partitions. *Annals of Mathematics*, 43(3):437–450, 1942. ISSN 0003486X. URL <http://www.jstor.org/stable/1968802>.
- [18] Friedman, D., Lampinen, A., Dixon, L., Chen, D., and Ghandeharioun, A. Interpretability illusions in the generalization of simplified models, 2023.
- [19] Fulton, W. and Harris, Joe. *Representation Theory*. Graduate Texts in Mathematics. Springer, New York, NY, October 1991. ISBN 978-0-387-97495-8.

- [20] GAP. Gap – groups, algorithms, and programming, version 4.12.2, 2023. URL <https://www.gap-system.org>.
- [21] Geiger, A., Potts, C., and Icard, T. Causal abstraction for faithful model interpretation, 2023.
- [22] Goldowsky-Dill, N., MacLeod, C., Sato, L., and Arora, A. Localizing model behavior with path patching, 2023.
- [23] Gromov, A. Grokking modular arithmetic, January 2023. URL <http://arxiv.org/abs/2301.02679>. arXiv:2301.02679 [cond-mat].
- [24] Guo, T., Hu, W., Mei, S., Wang, H., Xiong, C., Savarese, S., and Bai, Y. How do transformers learn in-context beyond simple functions? a case study on learning with representations, 2023.
- [25] Hase, P., Bansal, M., Kim, B., and Ghandeharioun, A. Does localization inform editing? surprising differences in causality-based localization vs. knowledge editing in language models, 2023.
- [26] Huang, J., Guestrin, C., and Guibas, L. Fourier Theoretic Probabilistic Inference over Permutations. *Journal of Machine Learning Research*, 10(37):997–1070, 2009. ISSN 1533-7928. URL <http://jmlr.org/papers/v10/huang09a.html>.
- [27] Jain, S. and Wallace, B. C. Attention is not explanation. In *North American Chapter of the Association for Computational Linguistics*, 2019. URL <https://api.semanticscholar.org/CorpusID:67855860>.
- [28] Karjol, P., Kashyap, R., and Ap, P. Neural Discovery of Permutation Subgroups. In *Proceedings of The 26th International Conference on Artificial Intelligence and Statistics*, pp. 4668–4678. PMLR, April 2023. URL <https://proceedings.mlr.press/v206/karjol23a.html>. ISSN: 2640-3498.
- [29] Kondor, R. and Trivedi, S. On the Generalization of Equivariance and Convolution in Neural Networks to the Action of Compact Groups. In *Proceedings of the 35th International Conference on Machine Learning*, pp. 2747–2755. PMLR, July 2018. URL <https://proceedings.mlr.press/v80/kondor18a.html>. ISSN: 2640-3498.
- [30] Kondor, Risi. *Group theoretical methods in machine learning*. PhD thesis, Columbia University, New York, NY, 2008. URL <https://dl.acm.org/doi/abs/10.5555/1570977>. Archive Location: world.
- [31] Kumar, T., Bordelon, B., Gershman, S. J., and Pehlevan, C. Grokking as the Transition from Lazy to Rich Training Dynamics, October 2023. URL <http://arxiv.org/abs/2310.06110>. arXiv:2310.06110 [cond-mat, stat].
- [32] Lieberum, T., Rahtz, M., Kramár, J., Nanda, N., Irving, G., Shah, R., and Mikulik, V. Does circuit analysis interpretability scale? evidence from multiple choice capabilities in chinchilla, 2023.
- [33] Liu, B., Ash, J. T., Goel, S., Krishnamurthy, A., and Zhang, C. Transformers Learn Shortcuts to Automata, May 2023. URL <http://arxiv.org/abs/2210.10749>. arXiv:2210.10749 [cs, stat].
- [34] Makelov, A., Lange, G., and Nanda, N. Is this the subspace you are looking for? an interpretability illusion for subspace activation patching, 2023.
- [35] Malandro, M. E. Fast Fourier transforms for finite inverse semigroups. *Journal of Algebra*, 324(2):282–312, July 2010. ISSN 0021-8693. doi: 10.1016/j.jalgebra.2009.11.031. URL <https://www.sciencedirect.com/science/article/pii/S0021869309006413>.
- [36] Malandro, M. E. Fourier Inversion for Finite Inverse Semigroups. *SIAM Journal on Discrete Mathematics*, 29(1):269–296, January 2015. ISSN 0895-4801. doi: 10.1137/130932028. URL <https://epubs.siam.org/doi/10.1137/130932028>. Publisher: Society for Industrial and Applied Mathematics.
- [37] McGrath, T., Rahtz, M., Kramar, J., Mikulik, V., and Legg, S. The hydra effect: Emergent self-repair in language model computations, 2023.
- [38] Merrill, W., Tsilivis, N., and Shukla, A. A Tale of Two Circuits: Grokking as Competition of Sparse and Dense Subnetworks, March 2023. URL <http://arxiv.org/abs/2303.11873>. arXiv:2303.11873 [cs].
- [39] Nanda, N. and Bloom, J. Transformerlens. <https://github.com/neelnanda-io/TransformerLens>, 2022.
- [40] Nanda, N., Chan, L., Lieberum, T., Smith, J., and Steinhardt, J. Progress measures for grokking via mechanistic interpretability. Technical Report arXiv:2301.05217, arXiv, January 2023. URL <http://arxiv.org/abs/2301.05217>. arXiv:2301.05217 [cs] type: article.

- [41] Nanda, N., Lee, A., and Wattenberg, M. Emergent Linear Representations in World Models of Self-Supervised Sequence Models, September 2023. URL <http://arxiv.org/abs/2309.00941>. arXiv:2309.00941 [cs].
- [42] O’Donnell, R. *Analysis of Boolean Functions*. Cambridge University Press, 2014. doi: 10.1017/CBO9781139814782.
- [43] OEIS Foundation Inc. The On-Line Encyclopedia of Integer Sequences, 2023. Published electronically at <http://oeis.org>.
- [44] Olah, C., Cammarata, N., Schubert, L., Goh, G., Petrov, M., and Carter, S. Zoom in: An introduction to circuits. *Distill*, 2020. doi: 10.23915/distill.00024.001. <https://distill.pub/2020/circuits/zoom-in>.
- [45] Olah, C., Cammarata, N., Schubert, L., Goh, G., Petrov, M., and Carter, S. Zoom In: An Introduction to Circuits. *Distill*, 5(3):e00024.001, March 2020. ISSN 2476-0757. doi: 10.23915/distill.00024.001. URL <https://distill.pub/2020/circuits/zoom-in>.
- [46] Plumb, G., Pachauri, D., Kondor, R., and Singh, V. SnFFT: A Julia Toolkit for Fourier Analysis of Functions over Permutations. *Journal of Machine Learning Research*, 16(107):3469–3473, 2015. URL <http://jmlr.org/papers/v16/plumb15a.html>.
- [47] Power, A., Burda, Y., Edwards, H., Babuschkin, I., and Misra, V. Grokking: Generalization Beyond Overfitting on Small Algorithmic Datasets, January 2022. URL <http://arxiv.org/abs/2201.02177>. arXiv:2201.02177 [cs].
- [48] Pyber, L. Enumerating finite groups of given order. *Annals of Mathematics*, 137(1):203–220, 1993. ISSN 0003486X. URL <http://www.jstor.org/stable/2946623>.
- [49] Rubin, N., Seroussi, I., and Ringel, Z. Droplets of Good Representations: Grokking as a First Order Phase Transition in Two Layer Networks, October 2023. URL <http://arxiv.org/abs/2310.03789>. arXiv:2310.03789 [cond-mat, stat].
- [50] Stein, W. et al. *Sage Mathematics Software (Version 10.0.0)*. The Sage Development Team, 2023. URL <http://www.sagemath.org>.
- [51] Steinberg, B. *Representation Theory of Finite Monoids*. Universitext. Springer International Publishing, Cham, 2016. ISBN 978-3-319-43930-3 978-3-319-43932-7. doi: 10.1007/978-3-319-43932-7. URL <http://link.springer.com/10.1007/978-3-319-43932-7>.
- [52] Varma, V., Shah, R., Kenton, Z., Kramár, J., and Kumar, R. Explaining grokking through circuit efficiency, September 2023. URL <http://arxiv.org/abs/2309.02390>. arXiv:2309.02390 [cs].
- [53] Vig, J., Gehrmann, S., Belinkov, Y., Qian, S., Nevo, D., Sakenis, S., Huang, J., Singer, Y., and Shieber, S. Causal mediation analysis for interpreting neural nlp: The case of gender bias, 2020.
- [54] Vink, R., Gooijer, S. d., Beedie, A., Gorelli, M. E., Zundert, J. v., Hulselmans, G., Grinstead, C., Santamaria, M., Guo, W., Heres, D., Magarick, J., Marshall, ibENPC, Peters, O., Leitao, J., Wilksch, M., Heerden, M. v., Borchert, O., Jermain, C., Haag, J., Peek, J., Russell, R., Pryer, C., Castellanos, A. G., Goh, J., illumination-k, Brannigan, L., Conradt, M., and Robert. pola-rs/polars: Python Polars 0.19.0, August 2023. URL <https://doi.org/10.5281/zenodo.8301818>.
- [55] Wang, K., Variengien, A., Conmy, A., Shlegeris, B., and Steinhardt, J. Interpretability in the wild: a circuit for indirect object identification in gpt-2 small, 2022.
- [56] Wei, J., Tay, Y., Bommasani, R., Raffel, C., Zoph, B., Borgeaud, S., Yogatama, D., Bosma, M., Zhou, D., Metzler, D., Chi, E. H., Hashimoto, T., Vinyals, O., Liang, P., Dean, J., and Fedus, W. Emergent abilities of large language models, 2022.
- [57] Xu, Z., Wang, Y., Frei, S., Vardi, G., and Hu, W. Benign Overfitting and Grokking in ReLU Networks for XOR Cluster Data, October 2023. URL <http://arxiv.org/abs/2310.02541>. arXiv:2310.02541 [cs, stat].
- [58] Zhang, S. D., Tigges, C., Biderman, S., Raginsky, M., and Ringer, T. Can Transformers Learn to Solve Problems Recursively?, June 2023. URL <http://arxiv.org/abs/2305.14699>. arXiv:2305.14699 [cs].
- [59] Zhong, Z., Liu, Z., Tegmark, M., and Andreas, J. The Clock and the Pizza: Two Stories in Mechanistic Explanation of Neural Networks, June 2023. URL <http://arxiv.org/abs/2306.17844>. arXiv:2306.17844 [cs].

A. Author Contributions

Dashiell Wrote the code for training and for calculating the Group Fourier Transform over S_n . Performed the initial analyses of models trained on S_5 and initially found what we came to call the coset circuit. Designed and ran causal interchange interventions. Derived formal properties of the coset circuit. Participated in discussions throughout the project and in writing the paper.

Qinan Ran training jobs and performed the bulk of circuit analysis on S_6 , designed and ran ablation experiments and causal interchange interventions, participated in discussions throughout the project and the writing of the paper.

Honglu Derived formal properties of the coset circuit, participated in the discussions throughout the project, and the writing of the paper.

Stella Helped scope the problem and identify and plan the core experiments. Advised on the interpretation of the analysis and the writing of the paper.

B. Experiment Details

We conducted experiments focusing on the permutation group of S_5 and S_6 .

Model	Epoch	Linear Layer Size	Embedding Size	Optimizer	Learning Rate
small	250,000	128	256	Adam	0.001
medium	250,000	1024	512	Adam	0.001
large	250,000	4096	512	Adam	0.001

Table 3. S_5 model information

Model	Epoch	Linear Layer Size	Embedding Size	Optimizer	Learning Rate
medium	200000	256	512	Adam	0.001
medium	200000	1024	512	Adam	0.001
large	200000	4096	512	Adam	0.001

Table 4. S_6 model information

C. Extra Graphs

C.1. Correlation of the Unembedding Vectors

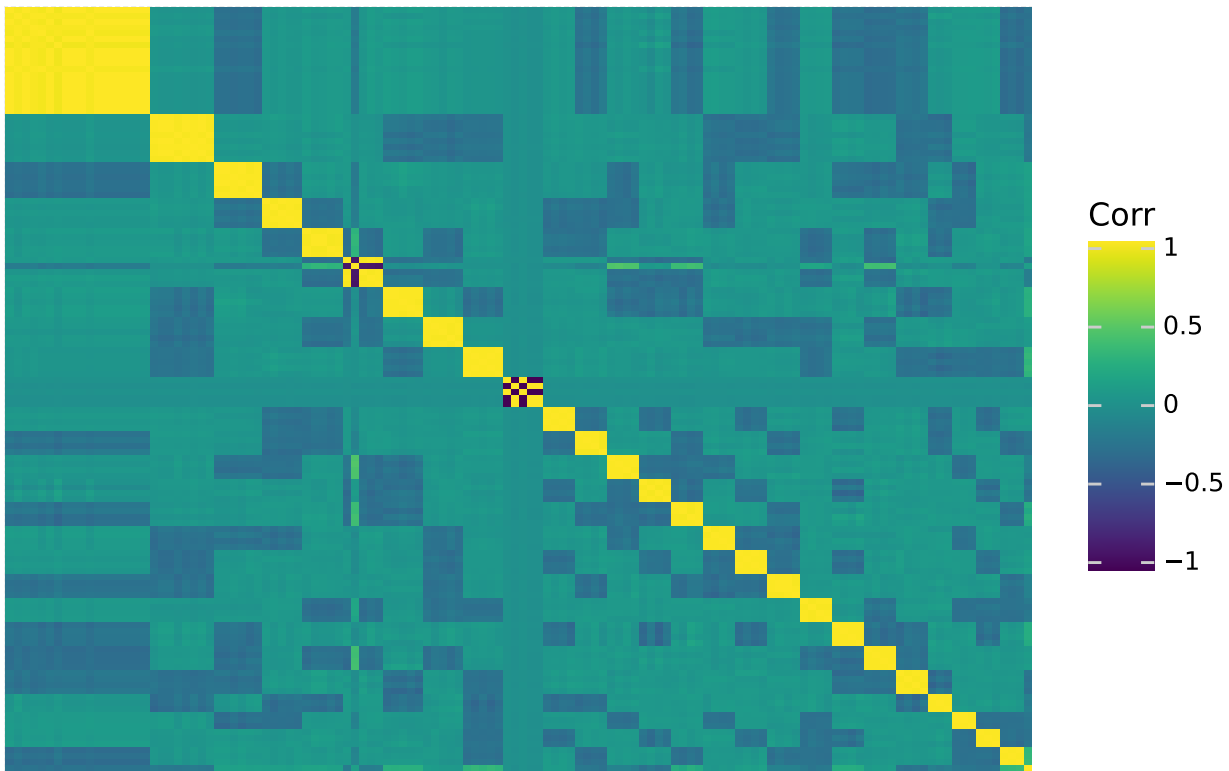


Figure 7. Correlation of the columns of an unembedding matrix, ordered so that columns that act on neurons of the same coset circuit type are next to each other. This illustrates both the amount of redundancy, as very few cosets only get a single neuron, and the degree to which the unembedding relies solely on constructive interference. The bulk of the action of the unembedding is just adding together the neurons from the same coset that have correlation near one. There are only two sets of neurons that exhibit destructive interference, which is identified by correlation near -1 .

C.2. (H_1, H_1) Circuit

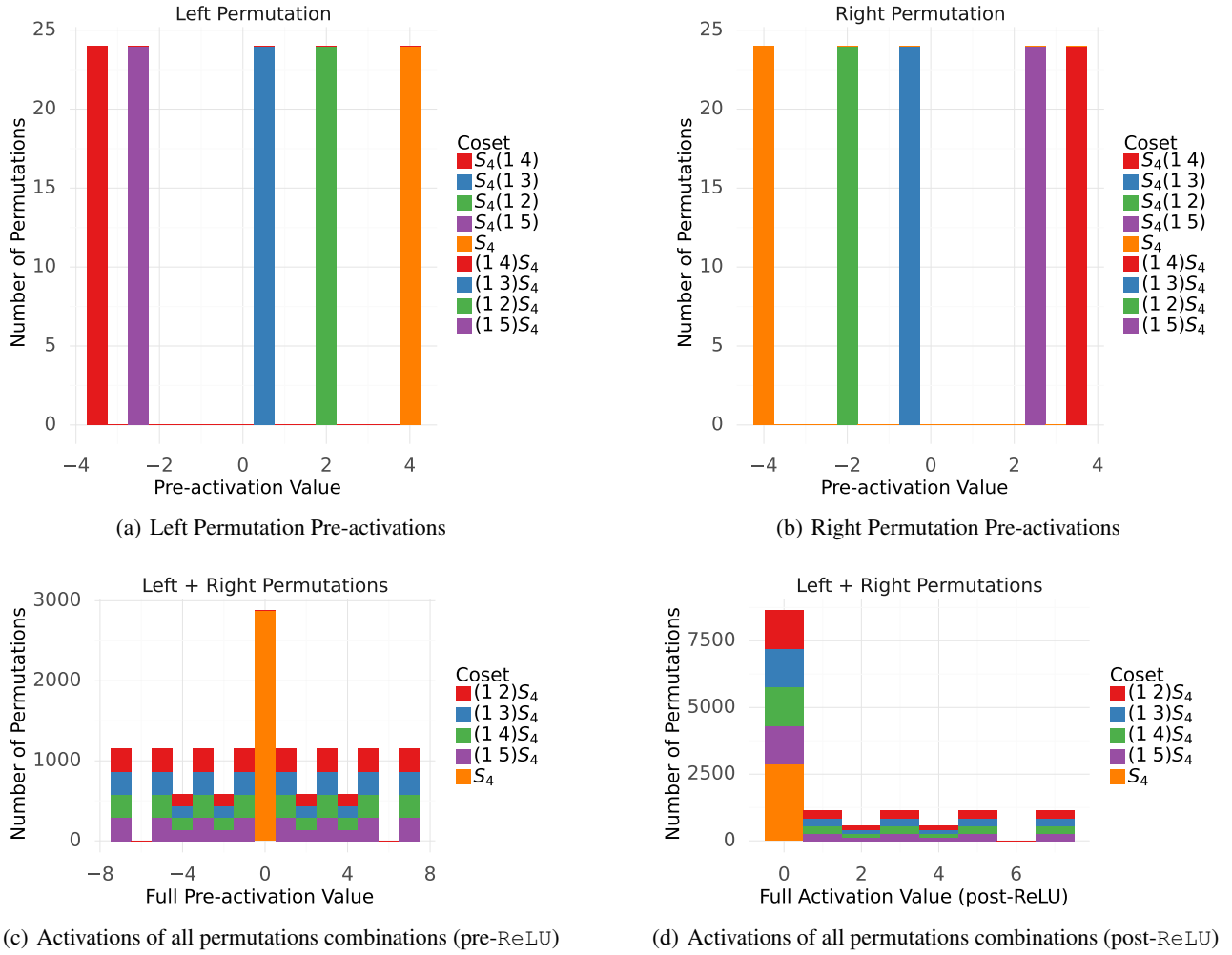


Figure 8. An example of a coset (H_1, H_1) circuit.

C.3. Distribution over Subgroups and Cosets

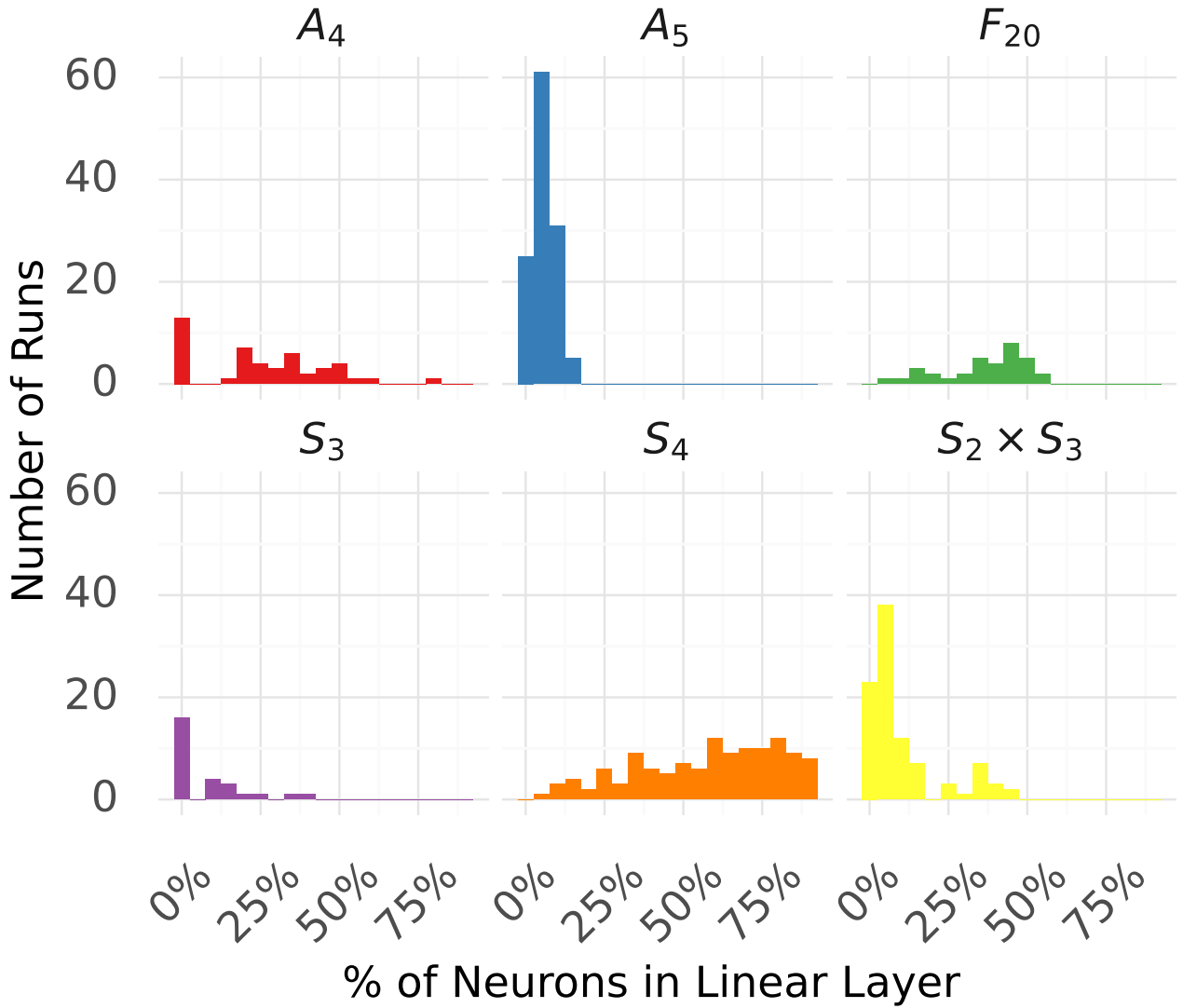


Figure 9. Distribution of coset circuits (as a percentage of neurons in the linear layer) for 128 runs trained on S_5 .

D. Group Theory

In this section, let us recall some basic definitions and propositions in group theory that are relevant to this paper.

D.1. Groups

A group G is a nonempty set equipped with a special element $e \in G$ called the *identity* and a multiplication operator \cdot satisfying the following:

- (inverse) For each element $a \in G$, there exists an element $b \in G$ such that $a \cdot b = b \cdot a = e$.
- (identity) For each element $a \in G$, $a \cdot e = e \cdot a = a$.
- (associativity) For elements $a, b, c \in G$, we have $(a \cdot b) \cdot c = a \cdot (b \cdot c)$.

The inverse of $a \in G$ is denoted by a^{-1} .

Example D.1. The set of integers \mathbb{Z} along with the addition $+$ form a group. The identity element is 0. Also with the addition, the same is true for the set of rational numbers \mathbb{Q} , the set of real numbers \mathbb{R} and the set of complex numbers \mathbb{C} .

Example D.2. The symmetric group introduced in Section 3.1 along with the composition of permutations satisfies the group axioms. The identity element is the identity permutation leaving each element unchanged.

Example D.3. The set of natural numbers \mathbb{N} and addition *do not* form a group. The reason being that the inverse elements do not exist except for 0.

Definition D.4. Given a group G , a subgroup H is a subset of G such that

- $a \cdot b \in H$ for any $a, b \in H$.
- $e \in H$.
- $a^{-1} \in H$.

One can check that H along with the multiplication satisfies the group axiom as well. H being a subgroup of G is denoted by $H \leq G$.

D.2. Cosets and double cosets

Definition D.5. Given a proper subgroup $H < G$ and an element $g \in G$, the set $gH := \{gh \mid h \in H\}$ is called a left H -coset. Similarly, $Hg := \{hg \mid h \in H\}$ is called a right H -coset.

gH is sometimes called a coset if the subgroup H is clear from the context. When we do not mention whether it is a left coset or a right coset, left coset is the default.

Lemma D.6. Two cosets g_1H and g_2H are either the same subset of G or disjoint (i.e., $g_1H \cap g_2H = \emptyset$).

Lemma D.7. If G is a finite group, any two H -cosets have the same number of elements.

As a result, one can pick suitable representative elements (but not unique) $g_1, \dots, g_n \in G$, so that g_1H, \dots, g_nH form a partition of G . Because the cosets have equal sizes, we can also conclude that $|G|$ is always divisible by $|H|$.

Definition D.8. Given two subgroups $H, L < G$ and an element $g \in G$, the set $HgL := \{hgl \mid h \in H, l \in L\}$ is called the (H, L) -double coset, or the double coset if the pair (H, L) is clear from the context.

Double cosets enjoy the similar property as cosets:

Lemma D.9. Two double cosets Hg_1L and Hg_2L are either the same or disjoint.

As a result, G can be similarly decomposed as a disjoint union of (H, L) -double cosets. However, when G is finite, (H, L) -double cosets do not always come with equal sizes. So the decomposition is not equal-sized.

For simplicity, we call the (H, H) -double coset the H -double coset.

D.3. Normal Subgroups

Definition D.10. A subgroup N is *normal* in G , denoted $N \trianglelefteq G$, if for any $g \in G$ and any $n \in N$, we have $gng^{-1} \in N$.

A subgroup is normal if and only if the left and right cosets are the same, i.e., for any $g \in G$, $gN = Ng$. Normal subgroups are important because they are precisely the groups for which the set of N -cosets G/N has a natural group structure.

Definition D.11. Given a group G and a normal subgroup $N \trianglelefteq G$, the *quotient group* G/N is defined to be the set of N -cosets endowed with the multiplication given by $gN \cdot hN = ghN$ for any $g, h \in G$.

The well-definedness of the multiplication is a consequence of N being normal and its group axioms are straightforward to check.

Example D.12. If G is commutative (for every $g, h \in G$, we have $gh = hg$), every subgroup $H \leq G$ is normal.

Example D.13. If $G = S_n$, the subgroup S_{n-1} fixing the first element is *not* a normal subgroup. On the other hand, the alternating subgroup A_n (consisting of even permutations) is a normal subgroup of S_n .

The double cosets of a normal subgroup is simply the usual cosets.

Lemma D.14. *Given a normal subgroup $H \trianglelefteq G$, the left H -coset and the right H -coset are in one-to-one correspondence. Furthermore, the set of H -double cosets is also in one-to-one correspondence to H -cosets.*

Proof. By definition, $gHg^{-1} = H$. Therefore, $gH = Hg$. $HgH = gHH = gH$. □

D.4. Conjugate Subgroups

The cosets of a normal subgroup $N \trianglelefteq G$ themselves form a group. If $x, y \in G$ and $x \in gN$ but $y \in hN$, then $xy \in ghN$. If G is not abelian, however, many or even all subgroups are not normal and do not have this property. For a non-normal subgroup H , a $g \notin H$ gives rise to a different conjugate subgroup gHg^{-1} .

In general, the relationship between the cosets of H and gHg^{-1} is complex, but they will have at least one left and one right coset in common: $Hg^{-1} = g^{-1}(gHg^{-1})$. Every right coset Hx will have a left coset pair $y(gHg^{-1})$ such that when multiplied, right coset on the left and left coset on the right, $Hxy(gHg^{-1}) = Hg^{-1}$, specifically when $xy = g^{-1}$.

This relationship between the cosets of pairs of conjugate subgroups is not as powerful as that of the cosets of normal subgroups, but conjugate subgroups are guaranteed to exist in non-abelian groups, whereas there are many simple groups without normal subgroups at all.

This relationship between pairs of conjugate subgroups is also useful enough that it is used by every model we trained. In general, we have the following:

Lemma D.15. *For any $H \leq G$ and an element $g \in G$, the set of conjugate elements gHg^{-1} forms a subgroup of G .*

If the conjugate subgroup gHg^{-1} is different than H , the left and right cosets gH, Hg are different.

The double coset circuits operate by first identifying a pair of different conjugate subgroups H and gHg^{-1} . It exploits the fact that the left coset gH and the right coset $(gHg^{-1})g$ are the same subset of G , which will be fully generalized and elaborated in the later sections.

D.5. An important case

When a group G decomposes as only two disjoint H -double cosets, any pair of subgroups conjugate to H shares a left coset with another's right coset.

Lemma D.16. *Let H_1, \dots, H_n be conjugate subgroups of G , such that for each H_i the double coset $H_i g H_i$ is equal to either H_i or $G \setminus H_i$. Then for each pair of subgroups H_i and H_j there exists a $g \in G$ such that $H_i g = g H_j$. Moreover, the only double cosets of H_i and H_j are $H_i g H_j = g H_j$ and $H_i x H_j = G \setminus g H_j$.*

Proof. If $i = j$, for any $h \in H_i$ the shared coset is the subgroup itself. If $i \neq j$, because H_i and H_j are conjugate, there exists a $g \in G$ such that $H_j = g^{-1} H_i g$. The left coset is equal to the right coset:

$$g H_j = g(g^{-1} H_i g) = H_i g$$

Notice that the double coset $H_i g H_j = H_i(H_i g) = H_i g$. But for $x \neq g$:

$$H_i x H_j = H_i x g^{-1} H_i g \tag{1}$$

$$= (G \setminus H_i) g \tag{2}$$

$$= G \setminus H_i g \tag{3}$$

□

D.6. Representation Theory

Definition D.17. Given a group G , a representation of G is a group homomorphism $\rho_V : G \rightarrow GL(V)$ for some finite (but nonzero) dimensional vector space V over a field k . When we do not specifically mention k , we use \mathbb{C} as the default.

In other words, a representation maps a group element g to a linear operator $f(g) : V \rightarrow V$ where V is a vector space of dimension d , so that the group multiplication becomes compositions of linear operators ($f(g \cdot h) = f(g) \circ f(h)$). Without explicit specifications, all representations in this paper are assumed to be over complex numbers.

When the context is clear, sometimes we omit the subscript V in the notation ρ_V .

The representations of finite groups have a rich and beautiful theory (see Diaconis [12], Fulton & Harris, Joe [19]). Here, we recall a few basic definitions and facts without going into details.

Definition D.18. A representation $\rho_V : G \rightarrow GL(V)$ is a sub-representation of $\rho_W : G \rightarrow GL(W)$ if V can be identified as a linear subspace of W so that $\rho_W(g)$ restricts to $\rho_V(g)$ for all $g \in G$.

Example D.19. For any group G , the map $G \rightarrow GL(V)$ sending all elements to the identity matrix is a representation. When $\dim(V) = 1$, we call it the *trivial representation* of G .

Definition D.20. Given two representations ρ_V, ρ_W of G , the direct sum of vector spaces $V \oplus W$ admits a natural representation of G by letting ρ_V, ρ_W act on each component separately. We call this the direct sum of representations ρ_V, ρ_W , and denote it by $\rho_V \oplus \rho_W$.

Definition D.21. Similarly, given two representations ρ_V, ρ_W , the tensor product $V \otimes W$ admits a natural representation of G by acting on V, W separately and extend by linearity. We call this the tensor product of representations ρ_V, ρ_W , and denote it by $\rho_V \otimes \rho_W$.

Definition D.22. A representation ρ of a group G is *irreducible*, if it does not have sub-representations other than ρ .

We denote the set of all irreducible representations of G by $\text{Irr}(G)$

Lemma D.23. A representation ρ of a finite group G is a direct sum of irreducible representations.

Example D.24. The trivial representation of G is irreducible.

Example D.25. The permutation representation maps $S_n \rightarrow GL(\mathbb{C}^3)$, i.e. 3×3 matrices with a single 1 in each row and column and zeros everywhere else.

$$(2\ 1\ 3) \mapsto \begin{pmatrix} 0 & 1 & 0 \\ 1 & 0 & 0 \\ 0 & 0 & 1 \end{pmatrix} \quad (3\ 2\ 1) \mapsto \begin{pmatrix} 0 & 0 & 1 \\ 0 & 1 & 0 \\ 1 & 0 & 0 \end{pmatrix}$$

You can see that the matrices of the permutation representation act on the basis vectors of \mathbb{C}^3 :

$$\begin{pmatrix} 0 & 0 & 1 \\ 0 & 1 & 0 \\ 1 & 0 & 0 \end{pmatrix} \begin{pmatrix} x \\ y \\ z \end{pmatrix} = \begin{pmatrix} z \\ y \\ x \end{pmatrix}$$

What it means to be a representation is that the group multiplication becomes matrix multiplication, so just as $(2\ 1\ 3)(3\ 2\ 1) = (2\ 3\ 1)$,

$$\begin{pmatrix} 0 & 1 & 0 \\ 1 & 0 & 0 \\ 0 & 0 & 1 \end{pmatrix} \begin{pmatrix} 0 & 0 & 1 \\ 0 & 1 & 0 \\ 1 & 0 & 0 \end{pmatrix} = \begin{pmatrix} 0 & 0 & 1 \\ 1 & 0 & 0 \\ 0 & 1 & 0 \end{pmatrix}$$

Example D.26. The permutation representation is *reducible*, because there is a subspace of the \mathbb{C}^3 that is invariant to its action.

$$\begin{pmatrix} 0 & 0 & 1 \\ 0 & 1 & 0 \\ 1 & 0 & 0 \end{pmatrix} \begin{pmatrix} x \\ x \\ x \end{pmatrix} = \begin{pmatrix} x \\ x \\ x \end{pmatrix}$$

Note that there is no permutation matrix acting on the vector $(x\ x\ x)^T$ that will change it, because all of the components are equal.

As it turns out, there are no *irreducible* representations of S_3 that are three-dimensional. The largest irrep of S_3 is $\rho_{(2,1)}$, which is made of 2×2 .

$$\begin{aligned} (2\ 1\ 3) &\mapsto \begin{pmatrix} -1 & 0 \\ 0 & 1 \end{pmatrix} \\ (3\ 2\ 1) &\mapsto \begin{pmatrix} \frac{1}{2} & -\frac{\sqrt{3}}{2} \\ \frac{\sqrt{3}}{2} & -\frac{1}{2} \end{pmatrix} \\ (2\ 3\ 1) &\mapsto \begin{pmatrix} -\frac{1}{2} & \frac{\sqrt{3}}{2} \\ -\frac{\sqrt{3}}{2} & -\frac{1}{2} \end{pmatrix} \end{aligned}$$

We leave it as an exercise to the reader to verify that $\rho_{(2,1)}(2\ 1\ 3)\rho_{(2,1)}(3\ 2\ 1) = \rho_{(2,1)}(2\ 3\ 1)$.

Trace is an important notion in linear algebra. Taking trace of a representation induces an important map from G to \mathbb{C} .

Definition D.27. Let ρ_V be a representation of G . The *character* of ρ_V is a map $\chi(\rho_V) : G \rightarrow \mathbb{C}$ given by $\chi(\rho_V)(g) = \text{tr}(\rho_V(g))$.

Lemma D.28. The character $\chi(\rho_V)$ takes the same value on a conjugacy class of G . In other words, $\chi(\rho_V)(h) = \chi(\rho_V)(ghg^{-1})$.

To distill this property for a wider range of functions, we have the following definition:

Definition D.29. Let $f : G \rightarrow \mathbb{C}$ be a map. If $f(h) = f(ghg^{-1})$ for any $g, h \in G$, f is called a *class function*.

For a finite group G , the set of class functions form a finite-dimensional vector space. There is an important inner product between class functions.

Definition D.30. The inner product of two class functions ϕ, ψ are defined as:

$$\langle \phi, \psi \rangle = \frac{1}{|G|} \sum_{g \in G} \phi(g) \overline{\psi(g)}.$$

As we require the class functions to take the same values on conjugacy classes, the dimension of the vector space of class functions is equal to the number of conjugacy classes in G . On the other hand, we have the following important theorem:

Theorem D.31. The characters of $\text{Irr}(G)$ forms an orthonormal basis in the vector space of class functions.

Lemma D.32. For a finite group G , $\text{Irr}(G)$ is a finite set. Furthermore, the order of $\text{Irr}(G)$ is equal to the number of conjugacy classes in G .

E. Fourier transform over finite groups

Despite being mostly perceived as a powerful tool in physics and engineering, the Fourier transform has also been successfully applied in group theory thanks to its generalization to locally compact abelian groups as well as an analog over finite groups. The purpose the group Fourier transform serves is largely analogous to the one served by the classical Fourier transform: it provides an alternate orthogonal basis with which to analyze functions from a group G to either \mathbb{R} or \mathbb{C} .

To motivate the transition from the classical Fourier theory to the Fourier theory over groups, we start with a brief recall of the definitions.

The classical Fourier transform over real numbers converts a complex-valued Lebesgue-integrable function $f : \mathbb{R} \rightarrow \mathbb{C}$ into a function from the complex unit circle S^1 to \mathbb{C} with following formula:

$$\hat{f}(\xi) = \int_{-\infty}^{\infty} f(x) e^{-2\pi i \xi x} dx. \tag{4}$$

Taking one step further in abstraction, we note that $e^{-2\pi i \xi x}$ as a function of x has the defining properties of turning additions into multiplications (being a group homomorphism) and always having complex norm 1:

$$\begin{aligned} e^{-2\pi i \xi (x_1 + x_2)} &= e^{-2\pi i \xi x_1} \cdot e^{-2\pi i \xi x_2}, \\ |e^{-2\pi i \xi x}| &= 1. \end{aligned}$$

We call such functions the *characters* of \mathbb{R} , though they are often thought of as *frequencies*. One can prove that all characters of \mathbb{R} can be written as $e^{-2\pi i \xi x}$ for a suitable $\xi \in \mathbb{R}$.

Looking back at (4), the properties we need in order to define the Fourier transform over \mathbb{R} are:

- \mathbb{R} has the Lebesgue measure (allowing for integration to happen).
- \mathbb{R} is a group (so that the characters make sense as group homomorphisms from \mathbb{R} to the unit circle group $S^1 \subset \mathbb{C}$).

Now, if we are given a finite group G , the Fourier transform of a finite group is an operator converting a map $f : G \rightarrow \mathbb{C}$ into a function between $\text{Irr}(G)$ and the set of linear operators $M(V)$.

Definition E.1. Given a group G , the *Fourier transform* of a map $f : G \rightarrow \mathbb{C}$ is a function \hat{f} from $\text{Irr}(G)$ to the union of $M(\mathbb{C}^n)$ for all n such that

$$\hat{f}(\rho) = \sum_{a \in G} f(a) \rho(a)$$

for an irreducible representation ρ .

The analogy comes from the following similar facts:

- G , as a finite set, has the invariant discrete measure (where the “integration” becomes the sum).
- G is a group, and the irreps ρ are in a sense the “smallest” group homomorphisms from G to $GL(n, \mathbb{C})$ (note that the images of ρ similarly have complex-norm-1 determinants due to G being a finite group).

For more details and applications, one can refer to, for example, [15]. We would like to note that there is also an inverse transform that restores the original function f from \hat{f} :

$$f(g) = \frac{1}{|G|} \sum_{\rho \in \text{Irr}(G)} d_\rho \text{tr}[\hat{f}(\rho) \rho(g^{-1})] \tag{5}$$

E.1. Projection on Fourier Basis

The inputs to the model are two one-hot vectors, x_l, x_r , which multiply the embedding matrices $E_l x_l$ and $E_r x_r$. E_l and E_r are $d \times |G|$ matrices, where d is the embedding dimension and $|G|$ is the size of the group. The *columns* are the embedding vectors for a single element $g \in G$. The normal approach would be to try and look at the column spaces of E_l and E_r , as these columns are the inputs to the model. However, since each *row* of E_l and E_r and each value of that row is associated with a single element of G , we instead treat each *row* of the embedding as a function $f : G \rightarrow \mathbb{R}$.

In fact, pretty much anywhere in the model where a matrix or set of activations has $|G|$ in the shape we can expand into the Fourier basis. For non-abelian groups, each Fourier frequency is an irrep, and the Fourier transform for each irrep is matrix-valued. This is, on its face, less than interpretable. Following the techniques outlined in Diaconis [12], however, we can expand the function at each element $g \in G$ into a new Fourier basis. Concretely, if our function $f : G \rightarrow \mathbb{R}$ is represented as a vector, we know from 5 that each element of the vector is a sum of the Fourier components:

$$\begin{bmatrix} f(g_1) \\ f(g_2) \\ \vdots \\ f(g_{|G|}) \end{bmatrix} = \frac{1}{|G|} \begin{bmatrix} \sum_{\rho} d_\rho \text{tr}[\hat{f}(\rho) \rho(g_1^{-1})] \\ \sum_{\rho} d_\rho \text{tr}[\hat{f}(\rho) \rho(g_2^{-1})] \\ \vdots \\ \sum_{\rho} d_\rho \text{tr}[\hat{f}(\rho) \rho(g_{|G|}^{-1})] \end{bmatrix}$$

We can keep track of all of the Fourier components at once by purposefully not completing the sum from 5), but instead keep each term into a new dimension:

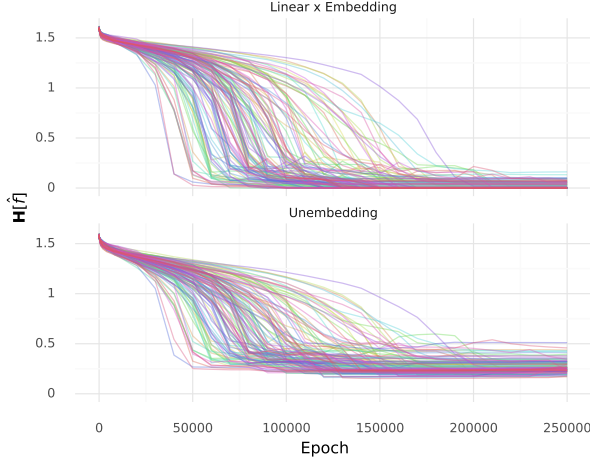


Figure 10. The evolution of the mean Fourier Entropy per layer over the course of training for 128 runs trained on S_5 . The maximum value $\mathbf{H}[\hat{f}]$ can take over S_5 is $\log(\frac{1}{7}) \approx 1.946$. $\mathbf{H}[\hat{f}] = 0$ implies that $\hat{f}(\rho) = 0$ on all but one irrep.

$$\frac{1}{|G|} \begin{bmatrix} d_{\rho_1} \operatorname{tr}[\hat{f}(\rho_1)\rho_1(g_1^{-1})] & \dots & d_{\rho_k} \operatorname{tr}[\hat{f}(\rho_k)\rho_k(g_1^{-1})] \\ d_{\rho_1} \operatorname{tr}[\hat{f}(\rho_1)\rho_1(g_2^{-1})] & \dots & d_{\rho_k} \operatorname{tr}[\hat{f}(\rho_k)\rho_k(g_2^{-1})] \\ \vdots & & \vdots \\ d_{\rho_1} \operatorname{tr}[\hat{f}(\rho_1)\rho_1(g_{|G|}^{-1})] & \dots & d_{\rho_k} \operatorname{tr}[\hat{f}(\rho_k)\rho_k(g_{|G|}^{-1})] \end{bmatrix}$$

Though this may seem like it is only making the data more complicated, it gives us many tools for analyzing the data. In particular, it turns out that the weights and activations are sparse in this new basis, which gives us a small path forward in analyzing the mechanisms.

Corollary E.2. *If H_i and H_j are conjugate subgroups of G such that the only two double cosets are $H_i g H_j$ and $H_i H_j$, then each right coset $H_i x$ has a paired left coset $y H_j$ where $y = x^{-1} g$ such that for all $h_x \in H_i x$ and $h_y \in y H_j$, $h_x h_y \in H_i g H_j$*

Lemma E.3. *Let $f : G \rightarrow \mathbb{C}$ be constant on the cosets of $H \leq G$ and non-zero on at least one coset. Then $\hat{f}(\rho) = 0$ if the restriction of ρ to H , $\rho|_H$ does not contain the trivial representation as a subrepresentation.*

Proof. The function f can be decomposed as the sum of functions

$$f_{xH}(\sigma) = \begin{cases} \alpha_x & \sigma \in xH \\ 0 & \text{otherwise} \end{cases}$$

for each coset xH . Because Fourier transform \hat{f} is invariant under translation we may, without loss of generality, analyze only the function f_H . For a given α_x , $\hat{f}_{xH}(\rho) = \hat{f}_H^x(\rho) = \rho(x) \hat{f}_H(\rho)$ for all $x \in G$. Recall the definition of $\hat{f}_H(\rho)$ from E.1:

$$\hat{f}_H(\rho) = \sum_{g \in G} f_H(g) \rho(g) \quad (6)$$

$$= \alpha_H \sum_{h \in H} \rho|_H(h) \quad (7)$$

$$= \alpha_H \sum_{h \in H} T^{-1} \left[\bigoplus_{\tau_i \in \mathcal{T}} \tau_i(h) \right] T \quad (8)$$

$$= \alpha_H T^{-1} \left[\bigoplus_{\tau_i \in \mathcal{T}} \sum_{h \in H} \tau_i(h) \right] T \quad (9)$$

where in 8 we decompose $\rho|_H$ into a direct sum of irreps of H . But because each τ_i is irreducible, $\sum_{h \in H} \tau_i(h) = \mathbf{0}$ unless τ_i is the trivial irrep. Thus, unless the decomposition of $\rho|_H$ into irreps of H includes the trivial representation, $\hat{f}|_H = 0$ \square

E.2. Logits and Counting Cosets

In Chughtai et al. [6], one way of justifying the GCR algorithm is to study the correlation between the character functions and the neuron activations. We would like to argue that the correlation between the GCR and the coset membership counting function may already exist, and in some simple cases it can be made explicit.

More precisely, we are measuring the correlation between the character function $\chi(\rho)$ of an irrep ρ with a set function $f : G \rightarrow \mathbb{C}$. In this section, we provide an explicit characterization of f in terms of trace and irreps, when f counts the membership of cosets.

We are specifically interested in the following situation:

Lemma E.4. *Suppose $f : G \rightarrow \mathbb{C}$ is a function such that its Fourier transform \hat{f} is nonzero only on an irreducible representation ρ and the trivial representation. Let $\hat{f}(\rho) = A \in M(\mathbb{C}^n)$. We have the following explicit formula:*

$$f(\sigma) = \frac{d_\rho}{|G|} \text{tr}(A \cdot \rho(\sigma^{-1})) + \frac{|H|}{|G|}. \quad (10)$$

Proof. This is immediate by the Fourier inversion formula. \square

In this case, although f is not directly written in terms of $\text{tr}(\rho(\sigma^{-1}))$, f is correlated with $\text{tr}(\rho(\sigma^{-1}))$ depending on how much A is concentrated to the diagonal and how even are the diagonal entries. For the rest of the section, we show that under certain conditions, Equation (10) applies verbatim to the functions that count membership of cosets for a collection of conjugate subgroups.

Given a subgroup $H \leq G$, let 1_H be the function that takes value 1 on the subgroup H , and takes 0 otherwise. The action of G on cosets G/H induces a representation of G on $\mathbb{C}^{|G/H|}$ by permuting the basis accordingly. We call it the *permutation representation* of G on G/H .

Lemma E.5. *The Fourier transform of 1_H is nonzero only at the irreducible components of the permutation representation of G on G/H .*

Proof. By definition, the Fourier transform of 1_H on an irrep ρ is

$$\widehat{1}_H(\rho) = \sum_{a \in H} \rho(a).$$

Notice that the image of $\sum_{a \in H} \rho(a)$ are invariant under H due to the symmetry of this expression.

Let V be the vector space where ρ acts on. Under the action of the subgroup H through ρ , one can decompose V as irreps of H . We group them into two parts:

$$V = V^H \oplus V',$$

where V^H is a direct sum of copies of trivial representation of H (or in other words, the invariant subspace of V under H), and V' is the direct sum of nontrivial irreducible components of V .

We immediately see the following by definition:

$$\sum_{a \in H} \rho(a)|_{V^H} = |H| \cdot \text{Id}_{V^H}.$$

Also by definition, nontrivial irreps of H do not have invariant subspaces since they do not admit proper sub-representations. Therefore,

$$\sum_{a \in H} \rho(a)|_{V'} = 0.$$

As a result, $\widehat{1}_H(\rho)$ is simply a scaled projection to the invariant subspace of V . Whether it is zero depends on whether $\text{Res}_H \rho$ has any trivial components.

By Frobenius reciprocity,

$$\langle \text{Ind}_H^G(1_H), \chi(\rho) \rangle = \langle 1_H, \chi(\text{Res}_H(\rho)) \rangle_H,$$

where $\chi(\rho)$ is the character of the irrep $\chi \in \text{Irr}(G)$ given by its traces, and $\langle \cdot \rangle$ is the inner product between class functions.

The left-hand side $\langle \text{Ind}_H^G(1_H), \chi(\rho) \rangle$ is nonzero if and only if ρ is an irreducible component of the permutation representation of G on G/H . The right-hand side $\langle 1_H, \chi(\text{Res}_H(\rho)) \rangle_H$ is nonzero if and only if $\dim(V^H) \neq 0$

□

Note that this lemma also works for 1_{gH} for a coset gH , since Fourier transforms turns the translation action by g into group multiplication by $\rho(g)$.

In the double coset circuit, we are specifically interested in the membership counting functions. More specifically, let H_1, \dots, H_n be a collection of conjugate subgroups of G . Given an element $\sigma \in G$, define the membership counting function as

$$F(\sigma) = \sum_{i=1}^n 1_{\sigma H_i}.$$

Combining all previous results, we have the following corollary describing the membership counting function F .

Corollary E.6. *If the permutation representation of G on G/H_1 has only 2 irreducible components, the Fourier transform \widehat{F} of the membership counting function F is nonzero only at these 2 irreducible components. In particular, the equation (10) applies to F .*

One may wonder how restrictive it is for the permutation representation on G/H to only have 2 irreducible components. The follow lemma shows that it applies to our case when $G = S_n$ and $H = S_{n-1}$.

Lemma E.7. *For S_n and the subgroup S_{n-1} fixing one element, the permutation representation has only two irreducible components.*

Proof. The natural representation of S_n on \mathbb{C}^n (by permuting the basis) decomposes as a direct sum of trivial representation and the standard representation of dimension $n - 1$. □

F. The Group Composition via Representations Algorithm

Our work and analysis owes much to "A Toy Model of Universality," though we come to different conclusions. Here we go over in detail the four main threads of evidence for the GCR algorithm that Chughtai et al. [6] put forward, which we restate here for clarity: (1) Correlation between the model's logits and characters of a learned representation ρ . (2) The embedding and unembedding layers function as a "lookup table" for the representations of the input elements $\rho(a)$, $\rho(b)$ and the inverse of the target $\rho(c^{-1})$. (3) The neurons in the linear layer calculate the matrix product $\rho(a)\rho(b) = \rho(ab)$. (4) Ablations showing that the circuit they identify is responsible for the majority of the model's performance. Though we were able to reproduce and verify almost all of Chughtai et al. [6]'s experimental results, we did not find evidence for the GCR algorithm. We instead found evidence that the models were encoding information about coset membership in their weights and, upon careful analysis, realized that the connections between functions from $S_n \rightarrow \mathbb{R}$ with low Fourier Entropy and the cosets of S_n provides an alternative explanation for the evidence that Chughtai et al. [6] provide.

F.1. Our Interpretation of the Evidence for GCR

Chughtai et al. [6] proposed as a hypothesis the "Group Composition via Representations" (GCR) algorithm in which the model encodes the group's irreducible matrix representations (irreps) in its weights and performs the requisite matrix multiplications to solve the task.

Although we replicated almost all of their analytical results, we could not confirm this hypothesis or find further evidence of the GCR algorithm. Close analysis revealed alternative explanations for data such as the observed sparsity in the group

Fourier basis and the correlation between the model’s logits and characters of irreps. We show that all of these observations are also consistent with the coset circuit we identify.

Ablations Though we do not perform all of the exact ablations that Chughtai et al. [6] perform, we also find that the weights that show high Fourier concentration and perform the coset multiplication are integral to the model’s performance, see Section 6.2.

Irrep Look Up Table We were not able to find any evidence that the embedding or unembedding layers function as a look-up table for any representation except for the one-dimensional sign representation. We did find that the model’s weights and activations *concentrate* on specific irreps in the group Fourier basis. This is due, however, to concentration on cosets of specific subgroups, not because the matrix representations are realized anywhere in the weights. The relationship between functions that are constant on cosets and specific irreps is shown in Appendix E.3.

Logit Attribution We also find that the model’s logits correlate with the character $\chi_\rho(abc^{-1})$ when the irrep ρ appears in the Fourier transform of the model’s weights. This is not, however, because the model has implemented the matrix product $\rho(ab)\rho(c^{-1})$, but because the model is counting the number of cosets that ab and c are both in. As we prove in E.2, if the cosets are of conjugate subgroups that have their Fourier transform concentrated on the irrep ρ (as we observe for the models in question), then the number of shared cosets will also correlate with the characters of ρ .

Matrix Multiplication of Irreps We were not able to find any evidence that the linear layer implements matrix multiplication, again excluding scalar multiplication of the sign irrep. Instead we show empirically that each neuron specializes in recognizing a pair of conjugate subgroups that have a set of shared cosets on which the group multiplication is simpler and predictable.

F.2. Evidence GCR Does Not Explain

Concentration on Cosets In the standard basis the pre-activations of the overwhelming majority of neurons concentrate heavily on the cosets of subgroups. This behavior is not predicted by the GCR algorithm.

The Difference Between Subgroups and Irreps We show that more than one subgroup of G may be have the Fourier transform of its indicator function concentrate on one irrep, such as S_{n-1} concentrating on entirely on $(n-1, 1)$. Additionally, as we see for subgroups of S_6 , many subgroups do not concentrate on only one irrep. This makes the assertion that there is a one-to-one relationship between irreps and circuits difficult to support, which at the least complicates GCR’s account of the mechanism.

Quantitatively speaking, the irreps (and therefore the GCR) already fail to catch up with the number of subgroups. Take S_n as examples, we have the following table ²:

	S_5	S_6	S_7	S_8	S_9	S_{10}	S_{11}	S_{12}	S_{13}
Number of subgroups	30	156	1455	11300	151221	1694723	29594446	404126228	10594925360
Number of irreps	11	19	56	96	296	554	1593	3094	10723

Table 5. The number of subgroups and the number of irreps from S_5 to S_{13}

Asymptotically, the number of subgroups of S_n is bounded below as follows (see [48, Corollary 3.3]):

$$2^{(\frac{1}{16} + o(1))n^2} \leq |\text{Sub}(S_n)|,$$

whereas the number of irreps of S_n is asymptotically the following (see [17]):

$$|\text{Irr}(S_n)| \sim \frac{1}{4n \cdot 3^{\frac{1}{2}}} e^{\pi(\frac{2}{3})^{\frac{1}{2}} n^{\frac{1}{2}}}.$$

We see that the former has a much higher asymptotic growth than the latter.

²The numbers of subgroups use the A005432 sequence of OEIS Foundation Inc. [43]. The numbers of irreps use the A000638 sequence of OEIS Foundation Inc. [43]

Unembedding Correlations of Neurons We observe that, except in the rare instances when a "positive" coset neuron forms, the correlation between neurons that concentrate on the same coset is $\approx 100\%$. The correlation between other neurons that concentrate on other cosets but are similar in Fourier space (have correlated irreps) only have 0 – 50% correlation.

Coset Circuit Specific Causal Interventions The property that the loss goes down when we replace the ReLU activation function with absolute value is a very strange property that GCR does not predict.

G. A Walkthrough of an S_4 Circuit

1. In the left embedding layer, encode which right coset of S_4^5 each permutation is in.
2. In the right embedding layer, encode which left coset of S_4^2 each permutation is in.
3. In the left linear layer, query the embeddings for the coset membership of σ_l . The pre-activations must only be dependent on the membership in the right cosets of S_4^5 . The left pre-activations are $\sigma_l \in S_4^5 \tau_{(i,5)} \mapsto x_{\tau_{i,5}}$.
4. In the right linear layer, query the embeddings for the coset membership of σ_r . The pre-activations must only be dependent on the membership in the left cosets of S_4^2 . The right pre-activations are, $\sigma_r \in \tau_{(2,j)} S_4 \mapsto x_{\tau_{(2,j)}}$.
5. The left and right pre-activations are added together, and again there are three options.
 - (a) If $\sigma_l \in S_4 \tau$ and $\sigma_r \in \tau S_4$ for the same transposition τ , then the pre-activation will be 0.
 - (b) σ_l and σ_r are not in matched cosets and $x_{\tau_l} + x_{\tau_r} > 0$. Then the neuron fires and the unembedding layer knows that $\sigma_l \sigma_r \notin S_4$
 - (c) σ_l and σ_r are not in matched cosets and $x_{\tau_l} + x_{\tau_r} < 0$. The ReLU will clip the negative pre-activation to 0.

H. Irreducible Representations

H.1. Symmetric Group S_5

For a subgroup $H \leq G$, we can investigate the Fourier transform of the indicator function 1_H by looking at its evaluation at each irrep. Concretely, we first center the indicator function by defining

$$f(g) = \begin{cases} -\frac{|H|}{|G|}, & g \notin H \\ 1 - \frac{|H|}{|G|}, & g \in H. \end{cases}$$

By doing so, \hat{f} evaluates to 0 on the trivial representation of G .

Given an irrep $\rho \in \text{Irr}(G)$, we first denote the value of the Fourier transform of f at ρ by $\hat{f}|_\rho$. The contribution of ρ to \hat{f} is defined by the following:

$$\frac{\|\hat{f}|_\rho\|^2}{\sum_{\delta \in \text{Irr}(G)} \|\hat{f}|_\delta\|^2}$$

Here, we list all the subgroups of S_5 and how each irrep of S_5 contributes to their indicator function. In the first column, we show the isomorphism type of each subgroup. Different subgroups can have the same isomorphism type. In the list:

- C_n means cyclic groups of order n .
- S_n means the symmetric group of n elements.
- A_n means the alternating group of n elements (the subgroup of S_n consisting of even permutations).
- D_{2n} means the n -gon dihedral group of order $2n$ (the symmetric group of regular polyhedron with n edges).
- F_{20} means the Frobenius group of order 20.

Isomorphism type	Generators	Size	(4, 1)	(3, 2)	(3, 1 ²)	(2 ² , 1)	(2, 1 ³)	(1 ⁵)
C_2	$\langle(12)\rangle$	2	20.3%	25.4%	30.5%	17%	6.8%	-
C_2	$\langle(12)(34)\rangle$	2	13.6%	25.4%	20.3%	25.4%	13.6	1.7%
C_3	$\langle(123)\rangle$	3	20.1%	12.8%	30.8%	12.8%	20.5%	2.6%
C_4	$\langle(1234)\rangle$	4	13.6%	25.4%	20.3%	25.4%	13.6%	1.7%
$C_2 \times C_2$	$\langle(12), (34)\rangle$	4	27.6%	34.5%	20.7%	17.2%	-	-
$C_2 \times C_2$	$\langle(12)(34), (13)(24)\rangle$	4	13.8%	34.5%	-	34.5%	13.8%	3.5%
C_5	$\langle(12345)\rangle$	5	-	21.7%	52.2%	21.7%	-	4.4%
C_6	$\langle(123), (45)\rangle$	6	21.1%	26.3%	31.6%	-	21.1%	-
S_3	$\langle(123), (12)\rangle$	6	42.1%	26.3%	31.6%	-	-	-
S_3^3	$\langle(123), (12)(45)\rangle$	6	21.1%	26.3%	-	26.3%	21.1%	5.3%
D_8	$\langle(1234), (13)\rangle$	8	28.6%	35.7%	-	35.7%	-	-
D_{10}	$\langle(12345), (25)(34)\rangle$	10	-	45.5%	-	45.5%	-	1%
$S_3 \times S_2$	$\langle(123), (12), (45)\rangle$	12	55.6%	44.4%	-	-	-	-
A_4	$\langle(12)(34), (123)\rangle$	12	44.4%	-	-	-	44.4%	11.2%
F_{20}	$\langle(12345), (2354)\rangle$	20	-	-	-	100%	-	-
S_4	$\langle(12345), (12)\rangle$	24	100%	-	-	-	-	-
A_5	$\langle(12345), (123)\rangle$	60	-	-	-	-	-	100%

Table 6. Subgroups of S_5 and the contribution of each irrep to their centered indicator function.